Atmos. Chem. Phys. Discuss., https://doi.org/10.5194/acp-2018-1325
Manuscript under review for journal Atmos. Chem. Phys.
Discussion started: 17 May 2019

Atmospheric Chemistry and Physics Discussions

Segregation in the Atmospheric Boundary Layer: The Case of *OH - Isoprene*

Ralph Dlugi[1,2,3], Martina Berger[1,2,3], Chinmay Mallik[2], Anywhere Tsokankunku[2,3], Michael Zelger[1,2,3], Otávio C. Acevedo[4], Efstratios Bourtsoukidis[2], Andreas Hofzumahaus[5], Jürgen Kesselmeier[3], Gerhard Kramm[6], Daniel Marno[2], Monica Martinez[2], Anke C. Nölscher[2], Huug Ouwersloot[2], Eva Y. Pfannerstill[2], Franz Rohrer[5], Sebastian Tauer[2], Jonathan Williams[2], Ana-Maria Yáñez-Serrano[3], Meinrat O. Andreae[3,7], Hartwig Harder[2] and Matthias Sörgel[2,3]

[1]Arbeitsgruppe Atmosphärische Prozesse (AGAP), Munich, Germany
[2]Atmospheric Chemistry Department, Max Planck Institute for Chemistry, P.O. Box 3060, 55020 Mainz, Germany
[3]Biogeochemistry Department, Max Planck Institute for Chemistry, Mainz, Germany
[4] Universidade Federal Santa Maria, Dept. Fisica, 97119900 Santa Maria, RS, Brazil
[5]Institut für Energie- und Klimaforschung: Troposphäre, Forschungszentrum Jülich, Germany
[6]Engineering Meteorology Consulting, Fairbanks, AK, USA
[7]Scripps Institution of Oceanography, University of California San Diego, California, USA

Correspondence to: R. Dlugi (rdlugi@gmx.de) and M.Sörgel (m.soergel@mpic.de)

Abstract

In the atmospheric boundary layer (ABL), incomplete mixing (i.e., segregation) results in reduced chemical reaction rates compared to those expected from mean values and rate constants derived under well mixed conditions. Recently, segregation has been suggested as a potential cause of discrepancies between modelled and measured OH radical concentrations, especially under high isoprene conditions. Therefore, the influence of segregation on the reaction of OH radicals with isoprene has been investigated by modelling studies and one ground-based and one aircraft campaign.

In this study, we measured isoprene and OH radicals with high time resolution in order to directly calculate the influence of segregation in a low-NO_x and high-isoprene environment in the central Amazon basin. The calculated intensities of segregation (I_s) at the Amazon Tall Tower Observatory (ATTO) above canopy top are in the range of values determined at a temperate deciduous forest (ECHO-campaign) in a high-NO_x low-isoprene environment, but stay below 10 %. To establish a more general idea about the causes of segregation and their potential limits, further analysis was based on the budget equations of isoprene mixing ratios,

the variance of mixing ratios, and the balance of the intensity of segregation itself. Furthermore, it was investigated if a relation of I_s to the turbulent isoprene surface flux can be established theoretically and empirically, as proposed previously. A direct relation is not given and the amount of variance in I_s explained by the isoprene flux will be higher the less the influence from other processes (e.g., vertical advection) is and will therefore be greater near the surface. Although ground based values of I_s from ATTO and ECHO are in the same range, we could identify different dominating processes driving I_s. For ECHO the normalized variance of isoprene had the largest contribution, whereas for ATTO the different transport terms expressed as a residual were dominating. To get a more general picture of I_s and its potential limits in the ABL, we also compared these ground based measurements to ABL modelling studies and results from an aircraft campaign. The ground based measurements show the lowest values of the degree of inhomogenous mixing (< 20 %, mostly below 10 %). These values increase if the contribution of lower frequencies is added. Values integrated over the whole boundary layer (modelling studies) are in the range from 10 % to 30 % and aircraft measurements integrating over different landscapes are amongst the reported. This presents evidence that larger scale heterogeneities in land surface properties contribute substantially to I_s.

1. Introduction

Reaction rates of atmospheric trace gases can deviate from the ones derived in laboratory experiments because the reactants might not be well mixed (i.e., they are segregated). Mixing in the atmospheric boundary layer (ABL) is provided by shear-generated turbulence or by convection. Therefore, mixing of the reactants will depend on the turbulence properties of the airflow. To achive well-mixed conditions, the mixing has to overcome the influences of heterogeneous source and sink distributions of the reactants due to fluxes into and out of the reaction volume and due to chemical reactions inside the volume. Thus, chemistry and turbulent properties need to be considered together (e.g., Seinfeld and Pandis, 1997; Finlayson-Pitts and Pitts Jr., 1986; Lamb and Seinfeld, 1973; Donaldson, 1975). Most models consider chemical reactions of first, second, and third order in a way that mean mixing ratios $\overline{c_i}$ and their products (e.g., $\overline{c_i} \times \overline{c_j}$ for a second-order reaction) together with the rate constant k_{ij} appear in the rate equations, as determined from laboratory experiments (e.g., Finlayson-Pitts and Pitts Jr., 1986). In the atmosphere, conditions often occur where the reactants are not well mixed with significant fluctuations, c_i' and c_j', compared to their mean values, $\overline{c_i}$ and $\overline{c_j}$. For those cases, also additional terms like variances and covariances, $\overline{c_i' c_j'}$, have to be considered (e.g., O'Brien, 1971; Lamb and Seinfeld, 1973; Shu,

1976; McRae et al., 1982; Donaldson and Hilst, 1972; Donaldson, 1975; Lamb and Shu, 1978). Here, c_i' and c_j' denote temporal fluctuations around the mean mixing ratios, $\overline{c_i}$ and $\overline{c_j}$, of compounds i and j, respectively. If for a second-order reaction the product of the mean mixing ratios fulfills the relation $\overline{c_i} \times \overline{c_j} \gg \overline{c_i' c_j'}$, the influence of turbulent fluctuating terms in the reaction rate equation $k_{ij}\left(\overline{c_i} \times \overline{c_j} + \overline{c_i' c_j'}\right)$ can be neglected for the prediction of either mean value, $\overline{c_i}$ or $\overline{c_j}$ (e.g., Danckwerts, 1952; Shu, 1976).

If this inequality is not valid, the balances of higher order moments (e.g., variances, covariances, triple correlations) have to be calculated either by the model or by analysis of experimental data. The quotient of the covariance term and the product of the means is commonly called the intensity of segregation, $I_s = (\overline{c_i' c_j'} / \overline{c_i} \times \overline{c_j})$ (e.g., Danckwerts, 1952; Damköhler, 1957) and is applied to describe the degree of inhomogeneous mixing for second order chemical reactions. For this Reynolds-type ensemble averaging of properties of a fluid, the influence of fluctuations on chemical reactions is described by additional differential equations to determine the higher-order moments (e.g., Donaldson and Hilst, 1972; Donaldson, 1973, 1975; Shu, 1976). Another way to approach this problem is to find the exact properties of the probability density functions of turbulent quantities for each reactant (e.g., O'Brien, 1971; Bencula and Seinfeld, 1976; Lamb and Shu, 1978).

The balance equation approach was also applied for the analysis of field measurements of the $O_3 - NO - NO_2$ system (e.g., Lenschow, 1982; Vilà - Guerau de Arellano et al., 1993; Kramm and Meixner, 2000) and to study segregation of the reaction of isoprene (ISO) with the hydroxyl radical (OH) (Dlugi et al., 2010, 2014). This concept not only considers the determination of first- and second- order moments (mean values, covariances and variances) but at least requires the additional knowledge of the third moments – e.g., the skewness, Sk (Stull, 1988; Sorbjan, 1989; Shu, 1976) - to quantify influences of so-called *coherent structures* (e.g., Katul et al, 1997, 2006; Raupach et al., 1996; Wahrhaft, 2000) on segregation (e.g., Dlugi et al., 2014).

Modelling studies on segregation for these chemical systems were mainly performed for more complex atmospheric mixtures (e.g., Schumann, 1989; Verver et al., 1997; Vinuesa and Vilà-Guerau de Arellano, 2005; Krol et al, 2000; Ouwersloot et al., 2011; Ebel et al., 2007; Patton et al., 2001; Kim et al., 2016; Li et al., 2016; Gerken et al., 2016) than could be considered by the analysis of field data (Dlugi et al., 2010, 2014; Kaser et al., 2015; Kramm and Meixner, 2000). Recently, the influences of shallow cumulus on transport, mixing and chemical reactions in the ABL were modelled for the reaction *isoprene + OH* (e.g., Vilà-

Guerau de Arellano et al., 2005; Ouwersloot et al., 2013; Kim et al., 2016; Li et al., 2016). The dynamics and mixing by shallow cumulus clouds are shown to enhance I_s also near the surface at least in qualitative agreement with the scarce experimental findings (Dlugi et al., 2014).

For a characterization of mixing and reaction conditions in atmospheric flows, the Damköhler number, Da_c, the quotient (τ_t/τ_c) between the characteristic timescales of turbulent or convective mixing processes, τ_t, and the specific chemical reaction, τ_c, of a compound (e.g., ISO or OH), is chosen (e.g., Vilá Guereau de Arellano and Lelieveld, 1998). This dimensionless number allows a classification of I_s as a function of nearly inert ($Da_c \ll 1$), slow ($0.05 \leq Da_c \leq 0.5$), fast ($0.5 \leq Da_c \leq 5$), and very fast ($Da_c > 5$) bimolecular reactions with respect to one of the two reactants. Damköhler numbers can be formulated in different ways in space and time, depending on the formulation of the turbulence scales (e.g., Donaldson and Hilst, 1972; Molemaker et al., 1998; Koeltzsch, 1998). Therefore, the actual numerical values of Da_c in various works found in the literature may differ systematically (e.g., Schumann, 1989; Sykes et al., 1994; Verver et al., 1997, 2000; Li et al., 2016). Nevertheless, the ranking of reactions being most influenced by inhomogeneous mixing is consistent within each choice of scales for the calculation of Da_c.

Some authors applied an additional scaling which uses the turbulent flux of a species (e.g.,$\overline{w'c_i'}$) at the surface to find a description for the reaction and inhomogeneous mixing (e.g., Schumann, 1989; Verver et al., 2000) and added a second Damköhler number, Da_f, to describe the influence of the surface flux on this ranking concept. This approach requires that for a specific reaction (e.g., $ISO + OH$) the segregation intensity, I_s, shows a clear functional dependence on the corresponding turbulent flux. We will therefore discuss this concept together with the theoretical framework applied to the analysis of the field data in Section 3. In Sections 3.4 and 4.1 we search for theoretical and empirical relations between the turbulent flux of isoprene and the related segregation intensity to test this hypothesis, because some studies suggest that spatially inhomogeneous distributions of emission fluxes significantly influence – in a direct relation - the segregation intensity (e.g., Krol et al., 2000; Pugh et al., 2011; Ouwersloot et al., 2011). The results from the aircraft measurements presented by Kaser et al. (2015) are interpreted in this way as well. They even suggest *a "feedback loop – the higher the isoprene flux the larger the I_s"*. The analysis of ECHO 2003 by Dlugi et al. (2014) showed that such an influence of spatially variable isoprene fluxes can be detected also in the results from measurements near canopy top, but needs a more specific interpretation (section 3.4).

One of the chemical reactions that has been studied experimentally is that of isoprene with OH radicals. Isoprene is an important biogenic compound with a global annual emission of $535\ Tg/a\ to\ 595\ Tg/a$ (Sindelarova et al., 2014; Guenther et al., 2012). If also the dependence on soil moisture stress is considered an annual emission of about $374 - 449\ T$ is estimated (Müller et al., 2008). Isoprene is emitted by various plants (Kesselmeier, 2001; Kesselmeier and Staudt, 1999; Günther et al., 1995). The emission source strength and related fluxes into the atmosphere are mainly controlled by plant physiological factors, absorbed radiation and leaf temperatures (e.g., Kesselmeier, 2001; Guenther et al., 2006; Ciccioli et al., 1997; Doughty, Goulden, 2008). After emission, isoprene is mixed by turbulence and convection in a cloud topped ABL (e.g., Heus and Jonker, 2008; Ramos da Silva et al., 2011; Ouwersloot et al., 2013), while being transported with the mean wind field. Isoprene reacts with OH (e.g., Finlayson-Pitts and Pitts Jr., 1986), the so called *detergent of the atmosphere,* which is formed by photochemical reactions and recycled in *radical chain reactions* (e.g., Finlayson – Pitts and Pitts, 1986; Rohrer et al., 2014). It is a fast reacting compound with $\tau_c < 1s$. Therefore, the hydroxyl radical (OH) is only locally determined by chemical sources and sinks which are influenced by the solar actinic flux, ozone (O_3), water vapor and additional reactants like HO_2, NO_2, NO, CO, CH_4 and various volatile organic compounds (VOCs). We may consider this chemical system in the way that isoprene (with $\tau_c > 300s$) is transported through this locally variable field of OH. Furthermore, the variability of the isoprene source strength in time and space (e.g., Ciccioli et al., 1997) – which may be described by the turbulent surface flux of isoprene $\overline{w'c_i'}$ - as well as of chemical sources and sinks of OH can contribute to the development of non-homogeneously mixed conditions with $I_s < 0$ (e.g., Krol et al., 2000; Ouwersloot et al., 2011; Dlugi et al., 2014). For the further analysis, the Damköhler number, Da_c, is used as a scale for the chemical reactant isoprene (ISO) with respect to the active species (OH).

This chemical system and its behavior in the ABL were analyzed by model studies for isoprene in a complex chemical mixture (Verver et al., 2000; van Stratum et al., 2012; Kim et al., 2016; Li et al., 2016). Patton et al. (2001) performed a Large Eddy Simulation (LES) study for isoprene in a mixture with CO to assess the influences of emission, mixing and reaction on the intensity of segregation, I_s, in the roughness sublayer (Raupach et al., 1996) within and directly above an idealized deciduous forest. All analyses found $I_s < 0$ near the bottom – e.g., canopy top - of their models, which is caused by an anti-correlation between the reacting compounds.

Ouwersloot et al. (2011) also applied LES to model mechanically and thermally generated turbulence above a differentially heated land surface representing alternating forest and

savanna areas. This inhomogeneity of land surface properties (and of canopy surface temperatures and surface sensible heat fluxes, H_s) is related to variations in buoyant production as well as inhomogeneous source distributions for isoprene, both of which have an impact on the variability of the isoprene flux and the mixing ratio (e.g., the variance) and, therefore, on I_s for the isoprene – OH reaction. Comparable to the study by Patton et al. (2001), the modelled chemical reactions are for low NO_x conditions as found for example in the Amazonian region (e.g., Rohrer et al., 2014) - where one major sink for OH is isoprene (e.g., Andreae et al., 2015; Karl et al., 2007; Nölscher et al., 2015; Yáñez- Serrano et al, 2015).

In their LES simulation, Kim et al. (2016) found that I_s is a function of the NO_x mixing ratio. They point out that values with $I_s < -0.1$ both for $NO_x < 0.2\,ppb$ and $NO_x > 1ppb$ are reached in a cloud layer. Positive values of I_s are calculated in the cloud layer for $NO_x \approx 0.5\,ppb$. In the mixed layer of the ABL Kim et al. (2016) found $I_s < -0.1$ only for $NO_x \geq 3\,ppb$. Their surface layer (SL) results are nearly independent from the NO_x mixing ratios with $-0.05 \leq I_s \leq 0.0$ for a homogeneous isoprene flux. In contrast, near the surface Ouwersloot et al. (2011) found significantly larger values for low NO_x- conditions, but in a region with inhomogeneous distributions of the surface sensible heat flux H_s and the isoprene emission flux $\overline{w'c_i'}$. In their Fig. 13 they show a case with $I_s = -0.195$ and $H_s \approx 0.15\,Kms^{-1}$ for an inhomogeneous distribution of the isoprene emission flux. But most of their results for homogeneous source distributions are in the range $I_s < -0.1$ and are at least qualitatively comparable to the results of Kim et al. (2016). The experimental values determined above canopy top during the ECHO 2003 field study with $NO_x > 1\,ppb$ are in the range $-0.16 < I_s \leq 0$ with the largest values determined for convective conditions in a cloud topped ABL (Dlugi et al. 2010, 2014).

Pugh et al. (2011) applied results from the field study ECHO 2003 (Dlugi et al., 2010) to estimate a potential influence of segregation for the reaction $ISO + OH$ on results of another field study above tropical rain forest in Indonesia, although the level of NO_x- compounds significantly differs from those at the deciduous forest of the ECHO site. For the Amazonian region, Butler et al. (2008) estimated that values of $-0.6 \leq I_s \leq -0.3$ are needed to interpret their chemical measurements with an aircraft in the upper ABL during the GABRIEL field campaign. But, after an extended error analysis, these authors estimated an average value of $I_s \approx -0.13$, about the largest value later on given by Dlugi et al. (2010, 2014) from direct measurements near the surface or by Ouwersloot et al. (2011) in their model study.

Dlugi et al. (2010, 2014) analyzed highly time-resolved ($\leq 0.2\ Hz$) data from measurements of isoprene and OH during the ECHO 2003 field experiment above a deciduous forest canopy in a polluted area (e.g., $NO_x > 1\ ppb$). They could specify influences of inhomogeneous source distribution, turbulence, and cloud-induced convective downward and upward transport on I_s in the range $-0.16 < I_s \leq 0$ for the reaction between isoprene and OH. In addition, they found for their experimental data that the time variation of the covariance between isoprene (c_i) and $OH(c_j)$, $d\left(\overline{c_i' c_j'}\right)/dt = S_{cov}$, was significantly smaller than all other terms in the prognostic equation for $\overline{c_i' c_j'}$. This allowed them to derive a diagnostic equation for I_s (based on the stationarity condition $S_{cov} = 0$) to separate influences of the complex interactions of mixing processes as a residuum (RE_{is}) from measurable quantities in the flow, like the normalized variance of isoprene, $nvar(ISO)$. Using this concept, they were able to compare their experimental findings with model results given by Ouwersloot et al. (2011) and Patton et al. (2001). They verified that $nvar(ISO)$ and RE_{is} both can be related to the influence of coherent motion near canopy top in a way that these terms correlate with the generalized correlation coefficient M_{21} for the turbulent transport of $nvar(ISO)$ as formulated by Katul et al. (1997) and Cava et al. (2006) by the third-order cumulant expansion method (CEM). I_s correlates not only with the (normalized) variance of isoprene but also with the turbulent flux of variance, and, therefore also well with the quantity $(nvar(ISO) - RE_{is})$ (Dlugi et al. 2014). In contrast, they found little to no correlation between I_s and the corresponding correlation coefficient M_{12} for the turbulent transport of the isoprene flux $\overline{w' c_i'}$ given by CEM. We refer to this result in Section 4.2.2.

Recently Kaser et al. (2015) published their results from the NOMADSS campaign on segregation in the system isoprene + OH from airborne measurements in the ABL for a flight level of about $z/z_i = 0.4$ (z = height above ground; z_i = ABL height). They determined a significant spatial variability of I_s during two flights (RF13, RF17). In addition, they presented LES model simulations in the range of $-0.35 < I_s \leq -0.06$ with a qualitative agreement with their experimental results near $z/z_i \approx 0.4$ but significantly larger values up to about $I_s \approx -0.4$ near the canopy top level compared to results from the other studies. Furtheron, they also suggest that a statistically significant relationship between the turbulent flux of isoprene $\overline{w' c_i'}$ and I_s exists. In addition, they stated that the covariance $\overline{c_i' c_j'}$ is directly proportional to I_s, which implies that the product of mean mixing ratios $\overline{c_i} \times \overline{c_j}$ is of minor influence.

In the following Section 2 we summarize the three field studies for which experimental data on segregation for the reaction *isoprene + OH* are available. These studies are ECHO 2003,

ATTO 2015 (see Sections 2.2, 3. and 4.), and NOMADSS (Kaser et al., 2015). In our discussion in Section 3 we present the theoretical frameworks, which serve as a rule on how to perform atmospheric measurements of this kind and to analyze the data. As introduction we give the definition of I_s and explain the different influences of the mean mixing ratios of $ISO(\overline{c_i})$ and $OH(\overline{c_j})$, their related standard deviations (σ_i,σ_j) and variances ($\overline{c_i'^2}$, $\overline{c_j'^2}$), their covariance ($\overline{c_i'c_j'}$) and the isoprene flux ($\overline{w'c_i'}$). For each of these quantities a prognostic balance equation (also named budget equation in the literature) allows us to analyze the impact of different processes on their behavior in time and space (e.g., Stull, 1988; Sorbjan, 1989; Seinfeld and Pandis, 1997). These processes are represented by the different terms of the balance equations as described for the exchange and transport of momentum, heat, and moisture for example by Monin and Obukhov (1954), Businger (1973), McBean and Miyake (1972), Panofsky and Dutton (1994), Stull (1988), Sorbjan (1989) or Garrett (1992) and for reacting compounds for example by Shu (1976), McRay et al. (1982), Lenschow (1982) or Ebel et al. (2007). This kind of analysis is done by solving these equations numerically in a model or by calculation of the different terms from direct measurements and order of magnitude estimates based on literature values, as also done in our study.

First, we perform such calculations for the balance of the mean mixing ratio $\overline{c_i}$ based on the data from ECHO 2003 and ATTO 2015 (Section 3.2). Secondly, we discuss the balances of the variances, as they can be directly related to the covariance, $\overline{c_i'c_j'}$, and to the segregation intensity, I_s (Section 3.3). In the following Section 3.4 we focus on the balance of the isoprene flux, $\overline{w'c_i'}$, to analyze if a direct relation to I_s can be established by a term of this equation, as suggested, for example, by Kaser et al. (2015). Finally, the balance of the segregation intensity, I_s, itself is evaluated based on measurements. In Section 4 we compare results from earlier modelling studies and direct field measurements near canopy top to each other and to the findings given by Kaser et al. (2015) from experiments in the ABL. The results from experiments in the atmosphere and modelling studies are compared also to obtain some empirical relation between the segregation intensity I_s and the Damköhler number Da_c.

2. The Field Studies

2.1. ECHO 2003

The ECHO intensive field campaign was performed from 17 June to 6 August 2003 on the grounds of the Reserch Center Jülich, Germany. Three towers were installed in a mixed deciduous forest with the dominating tree species, beech, birch, oak and ash, and a mean canopy height h_c of 30 m. The vertically integrated one-sided leaf area index in a radius of 50 m around the main tower varied between $LAI = 5.5$ and $LAI = 5.8$. The towers were aligned parallel to the main wind direction (Schaub, 2007) with the main tower in the center. The west tower was located 220 m from the main tower, and the east tower was located 120 m away. This allowed the investigation of the influence of the spatial distribution of biogenic volatile organic compound ($BVOC$) sources (isoprene, monoterpenes) on measured fluxes (e.g., Spirig et al., 2005). The field measurements were supported by the physical modelling of this forest site in a wind tunnel (Aubrun et al., 2005), also to estimate the influences of spatial heterogeneity of emission sources on measured fluxes of some $BVOCs$.

During the ECHO campaign, a feasibility study was performed on 25 July (day 206 of year 2003) to measure fluxes and higher order moments (e.g., covariances) not only for isoprene but also for the first time for OH- and HO_2- radicals. The data from these measurements were analyzed in detail for the time period between 09:00 and 15:00 CET. This period was characterized by cloudy conditions with a moderate horizontal wind velocity variation and slightly unstable to neutral stratification above the canopy. Broken cloud fields caused significant fluctuations of all radiation quantities above canopy. The air temperature, T_a, at the measuring height $z_R = 37\,m$ increased from 19 to 26.5 $°C$, while the specific humidity, q_a, increased only slightly from 09:00 to 12:00 CET from $8.3\,g\,kg^{-1}$ up to about $9.5\,g\,kg^{-1}$ and then decreased to about $8\,g\,kg^{-1}$ (Dlugi et al., 2010, 2014).

All measurements reported in the present paper were obtained at the main tower (Dlugi et al, 2010; 2014). The main tower with a height of 41 m, and the main measuring platform at $z_R = 37\,m$, was equipped with nine sonic anemometers/thermometers (METEK, instrument type: USA-1; time resolution 10 Hz) between 2 m and 41 m, and eight psychrometers (dry and wet bulb temperatures) at the same heights, except at 41 m. A time resolution for air temperature, T_a, and specific humidity, q_a, of $15\,s$ could be achieved. Radiation quantities and photolysis frequencies were obtained by radiometers directly above the canopy ($h_c = 30\,m$) with a time resolution of $3\,s$ (Bohn et al., 2004; Bohn, 2006; Bohn et al., 2006). Occasionally vertical profiles were measured.

The OH and HO_2 radical concentrations were measured by Laser Induced Fluorescence (LIF; Holland et al., 1995, 2003) on a vertically movable platform. For the reported measurements it was positioned above the canopy, with the inlet at 37 m height (Kleffmann et al., 2005). A proton-transfer-reaction mass spectrometer (PTR-MS) for measurements of isoprene, monoterpenes, methyl vinyl ketone (MVK), and methacrolein (MACR) was installed at the ground, using a sampling line to collect air at the height of the ultrasonic anemometer (Ammann et al., 2004; Spirig et al., 2005). The distances of the inlets of the PTR-MS and LIF instruments from the ultrasonic anemometer measuring volume were 0.45 m and 0.6 m, respectively. This spatial arrangement requires corrections to the calculated fluxes as outlined by Dlugi et al. (2010) and Dlugi et al. (2014). The time series of OH (and HO_2) and isoprene are available with a resolution of 0.2 Hz for the calculation of higher order mixed moments (e.g., covariances).

2.2. ATTO 2015

The ATTO-IOP1 was conducted at the Amazon Tall Tower Observatory (Andreae et al., 2015) in November 2015 (from 1 to 23 November) under El Niño conditions (Jiménez-Muñoz et al., 2016; Wang and Hendon, 2017). Measurements were made on an 80 m walk up tower at a height of $z_R = 41\ m$. The average canopy height, h_c, in the surroundings of the tower is around 35 m. The vertically integrated one-sided leaf area index (LAI) around the tower was about 6. The land cover in the main wind direction is primary rain forest with an extension of several hundred kilometers. During daytime, cumulus clouds develop regularely after noon.

Isoprene mixing ratios were measured by a PTR-MS at 1 Hz resolution. Air was drawn from the measurement height (41 m) by a 3/8-inch opaque fluorinated ethylene propylene (FEP) tubing at a rate of about 10 l min^{-1}. The line was isolated and heated. The inlet was protected by a 5 µm pore size Teflon filter. The time delay of the measured signal was corrected by maximizing the covariance between fluctuations of an open path H_2O analyzer (Licor 7500, Licor, USA) in front of the inlet and the signal of the water clusters inside the PTR-MS.

Atmospheric OH and HO_2 were measured during 16 – 23 November 2015 using a modified version of the HydrOxyl Radical measurement Unit based on fluorescence spectroscopy (HORUS) instrument (Martinez et al., 2010; Hens et al., 2014). The laser system was mounted on a cantilever balcony assembly at 36 m and the detection systems were mounted

Atmos. Chem. Phys. Discuss., https://doi.org/10.5194/acp-2018-1325
Manuscript under review for journal Atmos. Chem. Phys.
Discussion started: 17 May 2019

on another cantilever balcony at 40 m along with instruments to measure radiation, isoprene, and water vapour. The balcony faced to the north-east, the direction of the prevailing wind.

The measurements of atmospheric OH was achieved by measurements of the total OH signal, i.e., the signal produced due to fluorescence at 308 nm of atmospheric OH as well as of OH produced in the system during its travel time from the inlet nozzle to the detection volume, which we call background OH. The difference between the total signal and the background signal is thus a measure of atmospheric OH. The background OH can be measured by scavenging of the atmospheric OH with propane. The propane was introduced through an inlet pre-injector (IPI) mounted on top of the inlet nozzle (Novelli et al., 2014; Mao et al., 2012; Hens et al., 2014). During previous campaigns using the IPI system, the propane flow was switched on and off for two minutes each, providing a 4 minute time resolution for measurements of atmpospheric OH. For this campaign, we used an additional detection unit for simultaneous measurements of total and background OH in order to increase the time resolution of atmospheric OH measuremets. The detection unit for background OH was placed 55 cm to the east of the detection unit for total OH (Figure1).

Fig. 1 Set up of instruments and HORUS- inlets at $z_R \approx 41\ m$ at the ATTO tower during ATTO 2015. An inlet pre-injector is mounted on the inlet to the right side of the picture.

For measurement of HO_2 a second detection cell was mounted in series with the detection cell for total OH (without propane addition). NO was added in between the two measurement

cells to convert HO_2 to OH, which is then detected in the second cell (Hens et al., 2014; Mallik et al., 2018).

The laser system consisted of a tunable dye laser which was pumped by a diode-pumped Nd:YAG laser (Navigator I J40-X30SC-532Q, Spectra Physics) pulsing at 3 kHz. The 308 nm output laser radiation was split in a 3:1:3 ratio using beam splitters, and channeled through 5 m optical fibers into the three detection cells to measure total OH, HO_2 and background OH.

Ambient air was drawn into the inlets through critical orifices with pinhole sizes of 0.9 mm each into the respective detection cells below. The pinhole of the nozzles were 120 cm above the platform base at 40 m above ground level and about 10 m above the canopy. The internal pressure in the two OH detection cells, 4.5 ± 0.1 hPa, was maintained by two separate but identical pump systems mounted below the tower and connected to the respective detection systems by 50 m long (50 mm ID) tubes. The first pump system was used to draw in air for the total OH and HO_2 measurements and the second one for background OH.

The background OH was measured by titration with 12.5 cm^3 (STP) of pure propane in a carrier flow of 7000 cm^3 (STP) synthetic air. The scavenger amount was just sufficient to scavenge off ~95% of atmospheric OH as determined from propane titration experiments on-site. Initially, IPI systems were mounted on top of both the detection units, to be able to alternate measurements of of total and background OH measurements between the two units and characterize the losses occurring due to the IPI systems. The IPI systems were connected to a blower via a t-piece and individual valves adjusted for a flow of about 140 lpm of ambient air from the top of each IPI. The wall losses in the IPI were periodically determined by physically dismounting the IPI for 5 minutes during measurements during different times of the day.

For the measurement phase (19 - 23 Nov, 2015; day no: 323 (midday) - 327), the IPI was mounted only on the detection unit for background OH, providing us with a high time resolution for atmospheric OH measurements. In this phase, the scavenger was injected continuously resulting in measurements of total OH and background OH at a high time resolution of 15 s. The difference between these two signals gives a measure of the atmospheric OH at the same time resolution.

Calibration of the instrument for OH and HO_2 measurements was achieved by measuring the signals generated by known amounts of OH and HO_2 in a calibrator setup (Martinez et al.,

2010). The calibrator was mounted on top of the OH inlet without the IPI. Known amounts of OH and HO_2 were produced by irradiating different concentrations of humidified air with 185 nm radiation produced by a pen ray Hg lamp. The actinic flux density of the Hg lamp (Pen-ray line source, LOT-Oriel, Germany) used for the photolytic radical production was determined before and after the campaign using the actinometry method by N_2O photolysis (Martinez et al., 2010; Hens et al., 2014). The different OH and HO_2 mixing ratios were produced by mixing different combinations of humidified and dry air flows using mass flow controllers. The water mixing ratio in humid air stream was measured by a LICOR CO2/H2O-Analyzer (Li-7000).

2.3. NOMADSS – Field Study 2013

The Nitrogen, Oxidants, Mercury and Aerosol Distributions, Source and Sinks (NOMADSS) project was performed within the Southeast Atmosphere Study. NOMADSS consisted of three projects, one was the Southern Oxidant and Aerosol Study (SOAS). The results discussed by Kaser et al. (2015) are from flights conducted within SOAS by the National Center for Atmospheric Research's C130 aircraft in June / July 2013 in the central and southeast U.S. The complete planetary boundary layer budget of isoprene was measured (Kaser et al., 2015). Within these studies also the intensity of segregation for the reaction between isoprene and OH (Eq. (4)) was determined.

Isoprene was measured by a PTR-MS with a repetition rate of $> 1\ Hz$, during research flights RF13 and RF17. This time resolution is considered to be high enough to perform eddy covariance calculations for the isoprene flux $\overline{w'c_i'}$ and the covariance $\overline{c_i'c_j'}$ in Eq. (1) (e.g., Karl et al., 2013). In addition, a Trace Organic Gas Analyzer (TOGA) (e.g., Hornbrook et al, 2011) was applied also for measuring isoprene mixing ratios with a time resolution of about 2 minutes.

The HO_x- radicals, OH and HO_2, were detected using an ion chemical ionization mass spectrometer (Hornbrook et al, 2011; Mauldin III et al., 2003) as reported by Kaser et al. (2015; in text S3 of the supplement). Data for "OH were collected every 30 seconds", so that a time resolution of $0.033\ Hz$ was obtained. To generate OH data with higher time resolution Kaser et al.,(2015) "used spectral similarity conditions to reconstruct the spectral high-frequency loss based on concomitant fast isoprene and ozone measurements" both with time resolutions of $1\ s$, up to $5\ Hz$ sampling rate (see also Fig. S4 in Kaser et al., 2015).

In addition, observed and modelled isoprene surface fluxes were compared. The segregation intensity was modelled by the LES- code described by Patton et al. (2003) with the chemistry as given by Patton et al. (2001). Simulations were performed for homogeneous and heterogeneous (or inhomogeneous) land surface conditions, also to compare to results given by Ouwersloot et al. (2011).

3. Theoretical Concepts for Data Analysis

3.1. Introduction

Non-homogeneous mixing of chemically reactive compounds (i, j) causes a reduction of their mean reaction rates, $\overline{R_{ij}} = k_{ij} \times \overline{c_i} \times \overline{c_j}$, derived for homogeneous mixed conditions. Here, k_{ij} is the reaction rate constant, c_i, c_j are the specific mixing ratios, and the overbar denotes time averaged mean values (e.g., Seinfeld and Pandis, 1997).

As discussed before, for a second order reaction the influence of non-homogeneous mixing is commonly described by the intensity of segregation, I_s. This quantity is formulated in the sense of Reynolds (1895) and extended by Richardson (1920) for compressible fluids with all quantities α being a combination of their ensemble averages $\hat{\alpha}$ and the deviations $\tilde{\alpha}$ from that $\hat{\alpha}$. Here we replace $\hat{\alpha}$ by their timely averaged means $\overline{\alpha}$ and $\tilde{\alpha}$ by the deviation α' from $\overline{\alpha}$ (see Monin and Yaglom, 1971; Sorbjan, 1989 or Higgins et al., 2013 for further discussion). Therefore $\alpha = \overline{\alpha} + \alpha'$ and with the extension for mixing ratios, c_i and c_j, the reaction rate, R_{ij}, with the intensity of segregation, I_s, is given by (e.g., Astarita, 1967; O'Brien, 1971; Danckwerts, 1952; Donaldson, 1975; Lamb and Seinfeld, 1973; Shu, 1976):

$$R_{ij} = k_{ij} \times \overline{c_i} \times \overline{c_j} \left(1 + \frac{\overline{c_i' c_j'}}{\overline{c_i} \times \overline{c_j}}\right) = \overline{R_{ij}}(1 + I_s) \tag{1}$$

In general, a covariance $\overline{\alpha'\beta'}$ of two quantities α, β can be written as the product of the related standard deviations, σ_α and σ_β, times the correlation coefficient, $r_{\alpha\beta}$. For c_i, c_j this expression reads (Eq. (2))

$$\overline{c_i' c_j'} = r_{ij} \times \sigma_i \times \sigma_j \ , \tag{2}$$

at least if both quantities have probability density functions comparable to normal or log-normal distributions (Sachs and Hedderich, 2006). Combining Eq. (1) and Eq. (2) results in

$$I_s = r_{ij} \times \frac{\sigma_i \times \sigma_j}{\overline{c_i} \times \overline{c_j}} \quad (3)$$

with the covariance replaced by the product of terms on the right hand side of Eq. (2). Here results only of reaction (4)

OH + isoprene (ISO) → products (4)

are discussed, i.e., between a secondary compound, c_i (OH), and a primary, emitted compound, c_j (ISO). The depletion of the reacting compounds in Eq. (4) results in an anti-correlation between c_i and c_j. Consequently the covariance (Eq. (1) - Eq. (2)) and the correlation coefficient, r_{ij}, (Eq. (2) - Eq. (3)) become negative, which results in $I_s \leq 0$ in Eq. (1) and Eq. (3). Therefore, the reaction rate, R_{ij}, in Eq. (1) will be smaller than in the homogeneously mixed case, $(\overline{R_{ij}})$, as measured, e.g., under laboratory conditions to determine k_{ij} (e.g., Finlayson Pitts and Pitts, 1986).

Compounds like isoprene, but also other hydrocarbons, CO, CH_4, NO, or NO_2 are mainly emitted near the surface of the Earth. Other reactive compounds like OH (but also $C_xH_yO_z$ or O_3) are produced in the volume of the atmosphere in the course of chemical cycling (e.g., Seinfeld and Pandis, 1997; Rohrer et al., 2014).

In our discussion on the intercomparison of results from field and modelling studies for reaction Eq. (4) and of the influence of segregation, we have to analyze the multiple influences of the terms in Eq. (1) and Eq. (3) on I_s. Note that the turbulent vertical fluxes of compounds like c_i near the surface can be related to their emission rates (e.g., Guenther et al, 2006; Müller et al, 2008) at the surface E_i (e.g., from plants). E_{i0} is related to the turbulent surface flux $\overline{w'c_i'}|_0 = E_{io}$ and – in analogy to Eq. (2) – may be written as

$$E_{i0} \equiv \overline{w'c_i'} = r_{wc_i} \times \sigma_w \times \sigma_i \quad (5)$$

with the vertical wind velocity component w. If one formally replaces the standard deviation σ_i (e.g., for isoprene) in Eq. (3) by σ_i from Eq. (5), a relation where I_s is expressed also as function of the turbulent flux of compound c_i (Eq. (6)) can be formulated.

$$I_s = \underbrace{\left(\frac{r_{ij}}{r_w}\right)}_{1} \times \underbrace{\left(\frac{\overline{w'c_i'}}{\sigma_w \times \overline{c_i}}\right)}_{2} \times \underbrace{\left(\frac{\sigma_j}{\overline{c_j}}\right)}_{3} \quad (6)$$

Eq. (6) is composed of three terms:
(1) the ratio of the two correlation coefficients, (2) the ratio of the turbulent flux of compound c_i (here: ISO) and the product of the standard deviation of the vertical wind velocity component with the time average of the mixing ratio of c_i, and (3) the normalized standard

deviation of compound c_j (here: OH). All these quantities can be directly determined from high frequency measurements (e.g., $\overline{c_i}$, $\overline{c_j}$, $\overline{c_i'c_j'}$, σ_i, σ_j, $\overline{w'c_i'}$, $\overline{w'c_j'}$, …).

In models, prognostic (or balance) equations for any of these quantities (e.g., $\overline{c_i}$, $\overline{c_j}$, $\overline{c_i'c_j'}$, σ_i, σ_j, $\overline{w'c_i'}$, $\overline{w'c_j'}$, …) are solved to predict their behavior in time and space and their interactions. In this work, these quantities are calculated from direct measurements, or their order of magnitude is estimated to be able to determine which processes in the turbulent, convective atmospheric boundary layer (ABL) have the greatest influence on I_s.

Therefore, we need to consider how the I_s for reaction Eq. (4) could be related to the mean mixing ratios and the fluxes of the reactants ($\overline{w'c_i'}$, $\overline{w'c_j'}$), the variances ($\overline{c_i'^2}$, $\overline{c_j'^2}$) or other terms in the prognostic equations. We also need to briefly revisit the derivation of the diagnostic equation for I_s given by Dlugi et al. (2014), in order to clarify if a relation between the isoprene flux ($\overline{w'c_i'}$) and I_s can be established by the theoretical concept and to define the conditions under which experimental findings might also show such a relationship, i.e., a significant correlation between I_s and $\overline{w'c_i'}$. The following analysis is based on data from the field studies ECHO 2003 and ATTO 2015 and is compared to modelling results by Ouwersloot et al. (2011) and Patton et al. (2001) and also to findings described by Kaser et al. (2015) from the NOMADSS campaign.

We will examine the second-order equations that describe basic physical and chemical processes, which control the time behavior of the different input variables (mean mixing ratios, variances, co-variances) of Eq. (1) and Eq. (3) that are used to determine the intensity of segregation and finally the terms in the diagnostic equation for I_s itself. The product of the mean mixing ratios is the denominator in Eq. (1) and Eq. (3). The balances of the mixing ratios are described in the following section 3.2. The standard deviations (σ_i, σ_j) in Eq. (3) or Eq. (5) are given by the square roots of the variances. In Section 3.3 we therefore discuss which terms influence the variances of isoprene (or σ_i) and of OH. In Section 3.4 we also estimate terms of the balance of $\overline{w'c_i'}$ (i.e., the isoprene flux) and their relationship to Eq. (6). Finally various influences of different processes (chemistry and mixing) on the balance of I_s are discussed in Section 3.5.

3.2. Results for the Balance of the Mixing Ratios

The balance of the mean mixing ratios, $\overline{c_i}$, $\overline{c_j}$, is commonly analyzed by the corresponding prognostic equations (e.g., Stull, 1988). Here we shortly summarize the results discussed by Dlugi et al. (2014) on the balance of $\overline{c_i} = ISO$ and (where needed) on $\overline{c_j} = OH$. The balance for $\overline{c_i}$ is given by

$$S = \underbrace{\frac{\partial}{\partial t}\overline{c_i}}_{S} = -\frac{\partial}{\partial x_k}\left(\underbrace{\overline{u_k} \times \overline{c_i}}_{DMF} + \underbrace{\overline{u_k' c_i'}}_{DTF}\right) - k_{ij}\left(\underbrace{\overline{c_i} \times \overline{c_j}}_{MR} + \underbrace{\overline{c_i' c_j'}}_{TR}\right) \quad (7)$$

with $(x_1, x_2, x_3) = (x, y. z)$ for the coordinate axes, $(u_1, u_2, u_3) = (x, y. z)$ for the wind velocity components along these coordinate axes, and the other notation used as in Eq. (1) - Eq. (4). In Eq. (7) as well as the following equations, Einstein's summation convention is used. Dlugi et al. (2014) discussed the application of Eq. (7) for the ECHO 2003 study. The same concept is applied for the analysis of ATTO 2015.

The range of numerical values for the first term of Eq. (7) – commonly named *storage term* S - is given together with the computed results for MR and TR (MR = mean (time averaged) reaction rate between both compounds and TR = reaction rate of correlated turbulent fluctuating compounds (c_i', c_j')) together with the residuum given by DMF = divergence of the advective flux with the mean flow ($\overline{u_k}$) and DTF = divergence of the turbulent flux ($\overline{u_k' c_i'}$) in Table 1. Here k_{ij} is the reaction rate constant with an average value of $k_{ij} = 2.3\ ppb^{-1}s^{-1}$ for the reaction between isoprene and OH in the temperature range between 290 K and 300 K for both field studies. An averaging time interval for both field studies (ECHO 2003, ATTO 2015) of 10 minutes is selected to always fulfil conditions of stationarity during cloudy conditions at both field sites, as also discussed by Dlugi et al. (2010; 2014).

Tab. 1 The range of magnitude for all terms of Eq. (7) for isoprene in ppb s^{-1} for ECHO (25 July 2003) and ATTO (22 November 2015) with DMF+DTF determined as residuum.

Term	ECHO 2003	ATTO 2015
S	(-0.8 to 1.2)·10^{-3}	(-1.3 to 6)·10^{-3}
MR	(1 to 7)·10^{-4}	(1 to 9.5)·10^{-4}
TR	(0 to 7)·10^{-5}	(0 to 8)·10^{-5}
DMF +DTF	(-0.5 to 1.8)·10^{-3}	(-0.9 to 7)·10^{-3}

This analysis of data, for the isoprene balance from two field studies above the canopy top, shows that the term S (Eq. (7)) is balanced mainly by the divergence of the fluxes with a contribution of the mean reaction rate, MR, by about 10% or less and with $TR \leq 0.1\,MR$

(Table 1). During ATTO 2015, turbulent flux measurements for isoprene at height $z_R = 41\ m$ were performed. In addition, the related flux divergence is estimated based on measurements during ECHO 2003 proportional to the measured vertical gradient of the isoprene mixing ratio and the turbulent sensible heat flux divergence.

The term

$$DMF = \overline{u_k} \times \frac{\partial \overline{c_i}}{\partial x_k} + \overline{c_i} \times \frac{\partial \overline{u_k}}{\partial x_k} \tag{8}$$

is either calculated as a residuum (Table 1) or it can be estimated from the measured values at z_R and the vertical isoprene gradient. This latter method allows finding additional controlling parameters for $\overline{c_i}$, $\overline{c_j}$. The upward directed vertical turbulent fluxes of isoprene (emission flux) are in the range $0 < \overline{w'c_i'} < 0.3\ ppb\ m\ s^{-1}$ (25 July 2003) for ECHO and $0 < \overline{w'c_i'} < 1\ ppb\ m\ s^{-1}$ (22 November 2015) for ATTO. Note that for a mean upward directed vertical velocity $\overline{w} = 10^{-3} m\ s^{-1}$ (e.g., Stull, 1988), the mean vertical advective flux is in the range $10^{-3} \leq \overline{w} \cdot \overline{c_i} \leq 2 \cdot 10^{-2} ppb\ m\ s^{-1}$ for ATTO and smaller by up to an order of magnitude for ECHO. The accuracy of vertical velocity measurements during ECHO 2003 for the METEK USA1 ultrasonic anemometer is about $0.005\ m\ s^{-1}$ (Dlugi et al., 2010; 2014) and for ATTO 2015 (CSAT3) it is about $0.01\ m\ s^{-1}$. If $\overline{w}$ reaches values above $0.1\ m\ s^{-1}$ - for example during convective conditions - the fluxes with the mean flow become larger than the turbulent fluxes. Such conditions were observed during the case study of ECHO 25 July, 2003 (Dlugi et al., 2014) and also during the ATTO experiment on 22 November, 2015. Therefore, also the divergence of the mean flow (DMF) may be equal to or even larger than the divergence by the turbulent components (DTF) in Table 1. Measured values of DTF for isoprene from an aircraft campaign in California (different environment) are in the range of $2 - 3 \cdot 10^{-4}\ ppb\ s^{-1}$ with surface fluxes of the order of $0.3\ ppb\ m\ s^{-1}$ (Karl et al., 2013) while Su et al. (2015) reported surface fluxes around $1\ ppb\ m\ s^{-1}$ in the NOMADSS area. Note that the emission flux rate, E_{i0}, enters as the lower boundary condition if Eq. (7) is integrated along the z-coordinate. E_{i0} represents the *surface flux*, $\overline{w'c_i'}|_0$, as $\overline{w} = 0$ at leaf surfaces (e.g., Kramm, 1995; Müller et al., 2008). The flux divergence and not the flux itself controls $\overline{c_i}$. The sign of the divergence terms can be positive or negative. Therefore, only a change in dynamic conditions from convergence to divergence in the wind field with constant E_{i0} may significantly change S and potentially also MR and TR.

As a consequence, the surface flux, E_{i0}, the spatial distribution of the mean mixing rations, $\overline{c_i}$ and $\overline{c_j}$, but also of wind velocity components, ($\overline{u}$, $\overline{v}$, $\overline{w}$), are important for the time behavior of the mixing ratios in the atmosphere and near the canopy top. The balance of $\overline{c_j}$ above canopy top is only given by the chemical sinks and sources because mixing and advection

on a spatial scale above $1\,m^3$ are not relevant for a compound with $\tau_c < 1\,s$ and the terms DMF and DTF are zero. But compounds influencing the production or consumption of OH are advected to the measuring point and influence the magnitude and variability of S, MR, and TR.

Additionally, the segregation intensity, I_s, (Eq. (3)) is influenced by the standard deviations σ_i and σ_j. Patton et al. (2001) referred to the scalar variance budget and showed that second order reactions may act to destroy, but also to produce, variance of isoprene ($\sigma_i^2 = \overline{c_i'^2}$). We will therefore also discuss the balance of the variance in the following section 3.3.

3.3. Results for the Balance of the Variance

The analysis of terms of the balance equation of the covariance $\overline{c_i' c_j'}$ calculated from measurements during ECHO 2003 suggests that the normalized variance of isoprene can significantly influence I_s for the reaction of isoprene with OH (Dlugi et al., 2014). This agrees with earlier results of Patton et al. (2001) from LES modelling for an idealized forest, and, therefore, needs further consideration. Vinuesa and Vila-Guerau de Arellano (2005) introduced diagnostic equations for the variance of reactants in a CBL model and successfully predicted I_s as function of height for a reaction according Eq. (4). The balance equation for the variance of c_i - here for a divergence free wind field for simplification - reads (e.g., Stull, 1988, Sorbjan, 1989)

$$\underbrace{\frac{\partial}{\partial t}\overline{c_i'^2}}_{S_{var}} + \underbrace{\overline{u_k} \times \frac{\partial}{\partial x_k}\overline{c_i'^2}}_{A_{var}} + \underbrace{2 \times \overline{u_k' \cdot c_i'} \times \frac{\partial}{\partial x_k}\overline{c_i}}_{GP_{var}} + \underbrace{\frac{\partial}{\partial x_k}\overline{u_k' \cdot c_i'^2}}_{TT_{var}} + R_{var} + 2\varepsilon_{var} = 0 \qquad (9)$$

The first term denotes local storage of variance (S_{var}), the second term describes advection of spatial gradients of variance by the mean wind (A_{var}) while the third term is a production term caused by turbulent motions (turbulent fluxes of c_i) in a field with a mean gradient of $\overline{c_i}$ and is often called gradient production term (GP_{var}). Term four describes the turbulent transport of variance (TT_{var}), term five the chemical reactions (R_{var}) (see Eq. (10)) and term six is molecular dissipation (ε_{var}). The analyses of Schaub (2007), Aubrun et al. (2005), and Spirig et al. (2005) suggest that during ECHO 2003, isoprene is at least partly advected to the main tower from nearby trees (see also: Dlugi et al., 2014). Therefore, for the ECHO 2003 case, horizontal and vertical advection by the mean wind field, as described by the second term, A_{var}, may have significantly influenced the local mixing ratio $\overline{c_i}$ and the variance.

It was shown by model calculations by Schumann (1989), Patton et al. (2001), and Vinuesa and Vila-Guerau de Arellano (2005) that chemical reaction terms may be as large as other dynamic terms. The reaction term R_{var} in Eq. (10) reads

$$R_{var} = -2k_{ij}\left(\underbrace{\overline{c_i'^2} \times \overline{c_j}}_{I} + \underbrace{\overline{c_i'c_j'} \times \overline{c_i}}_{II} + \underbrace{\overline{c_i'c_i'c_j'}}_{III}\right) + J \times \overline{c_i'c_j'} \tag{10}$$

if a reversible reaction $c_i + c_j \rightarrow c_k$ (e.g., by photolysis of a product c_k with photolysis rate J) is possible. The fourth term in Eq. (10) does not apply for a reaction like $OH + isoprene$.

If stationarity conditions ($S_{var} = 0$) are considered, according to the experimental findings, which showed that this term sometimes is much smaller than others, another relation is given by the combination of Eq. (9) and Eq. (10). In such case the variance $\overline{c_i'^2}$ (occurring in term I of R_{var}) can be related to the sum of all other terms in a diagnostic form by

$$\overline{c_i'^2} = \frac{1}{k_{ij}\cdot\overline{c_j}}\left[\underbrace{\overline{u_k'c_i'} \times \frac{\partial}{\partial x_k}\overline{c_i}}_{GP_{var}} + \underbrace{\frac{1}{2}\overline{u_k} \times \frac{\partial}{\partial x_k}\overline{c_i'^2}}_{A_{var}} + \underbrace{\frac{1}{2}\frac{\partial}{\partial x_k}\overline{u_k'c_i'^2}}_{TT_{var}} + \varepsilon_{var} - k_{ij}\left(\underbrace{\overline{c_i} \times \overline{c_i'c_j'}}_{II} + \underbrace{\overline{c_i'c_i'c_j'}}_{III}\right)\right] \tag{11a}$$

A form for the vertical coordinate (z) only reads

$$\overline{c_i'^2} = \frac{1}{k_{ij}\cdot\overline{c_j}}\left[\underbrace{\overline{w'c_i'} \times \frac{\partial}{\partial z}\overline{c_i}}_{GP_{z,var}} + \underbrace{\frac{1}{2}\overline{w} \times \frac{\partial}{\partial z}\overline{c_i'^2}}_{A_{z,var}} + \underbrace{\frac{1}{2}\frac{\partial}{\partial z}\overline{w'c_i'^2}}_{TT_{z,var}} + \varepsilon_{var} - k_{ij}\left(\underbrace{\overline{c_i} \times \overline{c_i'c_j'}}_{II} + \underbrace{\overline{c_i'c_i'c_j'}}_{III}\right)\right]. \tag{11b}$$

In Eq. (6) the standard deviation for isoprene $\sigma_i = \left(\overline{c_i'^2}\right)^{1/2}$ is replaced by $\overline{w'c_i'} \cdot \left(r_{wc_i} \cdot \sigma_w\right)^{-1}$ according to Eq. (5) to formally relate I_s to the turbulent isoprene flux. Here the variance is related in an <u>additive</u> form to the turbulent flux in GP_{var} and to the covariance $\overline{c_i'c_j'}$ in I_s (Eq. (1)) by term II. Note that for a non-reactive scalar with $R_{var} = 0$ such diagnostic relations (Eq. (11a), Eq. (11b)) cannot be derived!

An order of magnitude estimation can be performed for all terms in Eq. (9), Eq. (11a), and Eq. (11b) to quantify which terms may have the largest impact on the variance. This calculation is based on results given by Dlugi at al. (2010, 2014) for ECHO 2003 and provided by Nölscher et al. (2016), Yanez-Serrano at al. (2015), and our own measurements (Section 2) for ATTO 2015 (Table 2).

1. The term $\left(k_{ij} \times \overline{c_j}\right)^{-1}$ is the chemical reaction time scale, τ_c, (with the average $k_{ij} = 2.3\, ppb^{-1}\, s^{-1}$; see section 3.2). For reaction Eq. (4) with $10^{-5} \leq [OH] \leq 5 \cdot 10^{-4}\, ppb$ this term is in a range of about 43.200 s (12h) to 650 s (0.18h). R_{var} (Eq.

(9)) is not larger than $10^{-3}\,ppb^2\,s^{-1}$ for ECHO 2003 and $3\cdot10^{-4}\,ppb^2\,s^{-1}$ for ATTO 2015 (22 November). On average the terms in Table 2 have to be multiplied by $\left(k_{ij}\times\overline{c_j}\right)^{-1}\approx 900\,s$ for ECHO 2003 and by $1900\ s$ for ATTO 2015.

2. The term GP_{var} is the product of the turbulent flux components and the spatial gradients of the mean isoprene mixing ratio, $\overline{c_i}$. The upward directed vertical turbulent fluxes of isoprene are in the range $0.02\,ppb\,m\,s^{-1}$ to $0.6\,ppb\,m\,s^{-1}$ (ECHO 2003) and $0\,ppb\,m\,s^{-1}$ to $1\,ppb\,m\,s^{-1}$ (ATTO; 22 November 2015). The measured vertical gradients of isoprene at the ECHO site are $0.01\,ppb\,m^{-1}$ to $0.05\,ppb\,m^{-1}$ and at the ATTO site $0.01\,ppb\,m^{-1}$ to $0.07\,ppb\,m^{-1}$ both for 10:00 – 16:00 LT and upward directed fluxes (see also: Nölscher et al., 2015; Yanez-Serrano at al., 2015). Note that large fluxes are sometimes also related to smaller gradients and smaller fluxes to larger gradients. Therefore a range of $8\cdot10^{-4}\le GP_{var}\le 10^{-3}\,ppb^2\,s^{-1}$ for ECHO 2003 and of $10^{-3}\le GP_{var}\le 3\cdot10^{-3}\,ppb^2\,s^{-1}$ for ATTO 2015 (November 22) is estimated.

3. For ECHO 2003, lateral and vertical advection of the isoprene mixing ratio $\overline{c_i}$ (DMF and DTF) are calculated to estimate the divergence of the fluxes in Eq. (7) (Table 1 and Dlugi et al., 2014). On average, the variance is $\overline{c_i'^2}\cong 0.42\,ppb^2$ and only larger by about 10% for increasing isoprene mixing ratios caused by horizontal advection as discussed by Dlugi et al. (2014). Vertical advection decreased $\overline{c_i}$ to $\overline{c_i}<0.4\,ppb$ but also decreased the variance to an average of $\overline{c_i'^2}\cong 0.13\,ppb^2$ in the downward transported air mass. With the average surface value being $\overline{c_i'^2}=0.42\,ppb^2$ and the value in the overlying part of ABL being $\overline{c_i'^2}=0.13\,ppb^2$, we estimate the origin of these air volumes to be around 300 – 400 m above ground (calculated from the difference in specific humidity and temperature). For an average $\overline{w}=-0.4\,m\,s^{-1}$ from measurements for these conditions, this term reaches values of about $A_{z,var}\cong 4{,}5\cdot10^{-4}ppb^2\,s^{-1}$ for the ECHO 2003 case.

For ATTO we obtain $\overline{c_i'^2}\approx 5.2\,ppb^2$ ($\overline{\sigma_i}\approx 2.5\,ppb$) for mean mixing ratios $\overline{c_i}\approx 7\,ppb$ after noon with comparable $\overline{w}$ and percentage changes of variance during downdrafts. Therefore, this term is estimated to be of the same magnitude during ATTO 2015 as for ECHO 2003. The horizontal advection term for ECHO 2003 can be estimated with $\overline{u_H}=2\,m\,s^{-1}$ and $\Delta\overline{c_i'^2}\cong 0.04\,ppb^2$ from measurements at a distance of about 125 m between the west tower and the main tower (Dlugi et al., 2010; 2014)

to be $A_{h,var} \cong 8 \cdot 10^{-4} ppb^2\, s^{-1}$. The observed change of variance during horizontal advection for ECHO 2003 is small. If we assume comparable conditions for the ATTO field site a magnitude of the horizontal advection of $A_{h,var} \approx 10^{-3} ppb^2\, s^{-1}$ is determined.

For ECHO 2003, the vertical turbulent transport of isoprene variance is calculated from measurements as $\overline{w' c_i'^2} \leq 10^{-2} ppb^2\, m\, s^{-1}$. The analysis of terms of the variance balance equations for potential temperature and of isoprene on day 200 – 206 of ECHO 2003 shows, that TT_{var} for both quantities θ and ISO are proportional to each other. We assume that the percentage vertical change of TT_{var} is comparable to the change of the same term for temperature variance also on day 206 (25 July 2003), when the ECHO 2003 case study on segregation (Dlugi et al., 2010; 2014) was performed, and obtain $TT_{var} \approx 5 \cdot 10^{-4} ppb^2\, s^{-1}$. With the same relation we estimate $TT_{var} < 10^{-3} ppb^2\, s^{-1}$ for ATTO 2015 (25 November 2015).

4. For the ECHO 2003 case the covariance in term II (Eq. 11a, 11b) is in the range $0 < \left|\overline{c_i' c_j'}\right| < 3 \cdot 10^{-5} ppb^2$ (see also Fig. 12 in Section 4.2.1 and Fig. 8 in Dlugi et al., 2014) with the average mixing ration $\overline{c_i} \approx 0.7\, ppb$. Therefore, for the ECHO 2003 study, term II is smaller than $2 \cdot 10^{-5} ppb^2\, s^{-1}$ and term III is $< 10^{-6} ppb^2\, s^{-1}$ (see also Fig. 12 in Dlugi et al., 2014). Both terms are comparable in magnitude during ATTO 2015 (November 22, 2015). Table 2 summarizes these estimates.

5. Molecular dissipation (Sorbjan, 1989) is often determined by

$$\varepsilon_\alpha = \nu_\alpha \overline{\left(\frac{\partial \alpha'}{\partial x_k}\right)^2}$$

for any quantity α (ν_α = kinematic molecular diffusivity for α in air). For the ECHO 2003 case and for $\alpha \equiv c_i = ISO$, the kinematic molecular diffusivity is of order $10^{-5} m^2\, s^{-1}$ and the gradient of fluctuations is about $10^{-2} ppb\, m^{-1}$ from measurements on days 200 – 203, 2003 (see above) (Dlugi et al., 2014). Therefore, an order of magnitude estimate is $\varepsilon_{var} \approx 10^{-9} ppb^2\, s^{-1}$. Even for a gradient 10^2 times larger (e.g., of about $1\, ppb\, m^{-1}$), we get $\varepsilon_{var} < 10^{-4} ppb^2\, s^{-1}$.

These results show that conditions exist above canopy top where the *gradient production,* GP_{var}, becomes the largest term in the variance balance. Then the magnitude of $\overline{c_i'^2}$ is mainly determined by GP_{var} but with some significant contribution of variance advection A_{var} and TT_{var} (see Table 2), if Eq. (11a), Eq. (11b) are

Atmos. Chem. Phys. Discuss., https://doi.org/10.5194/acp-2018-1325
Manuscript under review for journal Atmos. Chem. Phys.
Discussion started: 17 May 2019

approximately valid. In Section 4, we will discuss these findings together with the question if I_s can be simply expressed by a proportionality to the turbulent isoprene flux, $\overline{w'c_i'}$.

Tab. 2 The estimation for the magnitude of terms in the diagnostic equations (Eqs. 11a, 11b) for the isoprene variance during ECHO 2003 (25 July, 2003) and ATTO 2015 (25 November, 2015) in $[\boldsymbol{ppb^2\ s^{-1}}]$.

Term	ECHO 2003	ATTO 2015
GP_{var}	$8 \cdot 10^{-4}$ to 10^{-3}	10^{-3} to $3 \cdot 10^{-3}$
$A_{h,var}$	$\approx 8 \cdot 10^{-4}$	assumed to be $\approx 10^{-3}$
$A_{z,var}$	$\approx 4.5 \cdot 10^{-4}$	$\approx 4.5 \cdot 10^{-4}$
TT_{var}	$\approx 5 \cdot 10^{-4}$	assumed to be $< 10^{-3}$ (see text)
II	$\leq 4 \cdot 10^{-5}$	$\leq 4 \cdot 10^{-5}$
III	$\leq 10^{-6}$	$\leq 10^{-6}$

3.4. Results for the Balance of the Isoprene Flux

The balance of the isoprene flux is discussed in comparison to experimental results from the field (ECHO 2003: Dlugi et al., 2010, 2014; ATTO 2015: see also Section 4). As an example, we mainly focus on results from the ECHO 2003 campaign but also refer to ATTO 2015.

The vertical turbulent fluxes of reactive compounds like isoprene (ISO) and OH varied with time during 25.07.2003 (DOY 206) of ECHO 2003 (Dlugi et al., 2010). Eq. (12) describes the behavior of the vertical flux (without the influence of advection with the mean flow velocity) for a component i and has different terms besides the reaction term R_{wi} (e.g., Patton et al., 2001, Verver et al., 2000).

$$\underbrace{\frac{\partial}{\partial t}\overline{w'c_i'}}_{S_{wi}} = \underbrace{-\overline{w'^2} \times \frac{\partial \overline{c_i}}{\partial z}}_{i} + \underbrace{\frac{g}{\theta_{v_0}} \times \overline{c_i'\theta_v'}}_{ii} - \underbrace{\frac{\partial}{\partial z}\overline{c_i'w'w'}}_{iii} - \underbrace{\frac{1}{\rho} \times \overline{c_i'\frac{\partial p'}{\partial z}}}_{iv} + \underbrace{R_{wi}}_{v} - \underbrace{2\varepsilon_{wi}}_{vi} \tag{12}$$

$$R_i = -k_{ij}\left(\underbrace{\overline{c_i} \times \overline{w'c_j'}}_{I} + \underbrace{\overline{c_j} \times \overline{w'c_i'}}_{II} + \underbrace{\overline{w'c_i'c_j'}}_{III}\right) \tag{13}$$

Here, g is the acceleration of gravity, θ_v is the virtual potential temperature, p is the air pressure. The reaction term in Eq. (13) is composed of the product of mean mixing ratios with vertical fluxes (I: of OH; II of ISO) and of the turbulent transport of the covariance – the numerator of I_s of both reactants (see Eq. 1). All terms in Eq. (13) can be calculated from measurements, while the other terms in Eq. (12) can be estimated as discussed in the following.

For the reaction $ISO + OH$ (Eq. 4) the following order of magnitude estimation for terms in Eq. (13) shows that most terms cannot be neglected a priori.

- The first term (I) in Eq. (13) is the product of the mean concentration of isoprene (in the range of $0.1 - 2.5\,ppb$ for ECHO 2003 and $0.3 - 18\,ppb$ for ATTO 2015 (Section 2) with the turbulent flux of OH (in the range of about $10^{-5} - 5 \cdot 10^{-5}\,ppb\,m\,s^{-1}$) for both field experiments. The turbulent OH flux is often set to zero (e.g., Kaser et al., 2015), although the numerical value is significant. This flux is the result of the in-flux and out-flux of other chemical compounds which act as sinks and sources in a small volume of the order $< 1\,m^3$ where the OH radical is locally detected. Due to its short lifetime (< 1 sec) OH is just transported on scales of a few centimeters. Considering a mean value of $k_{ij} = 2.3\,ppb^{-1}\,s^{-1}$ for reaction Eq. (4) this first term (I) varies in a range of $4 \cdot 10^{-6} - 2.3 \cdot 10^{-3}\,ppb\,m\,s^{-2}$.

- The mean OH mixing ratio for ECHO 2003 is between about $10^{-4}\,ppb$ and $5 \cdot 10^{-4}\,ppb$ (with higher values up to $7 \cdot 10^{-4} ppb$) and the turbulent isoprene flux varies between about $0.02\,ppb\,m\,s^{-1}$ and $0.6\,ppb\,m\,s^{-1}$ (Spirig et al., 2005; Dlugi et al., 2010). This results in $10^{-6}\,ppb\,m\,s^{-2}$ to $4.2 \cdot 10^{-5}\,ppb\,m\,s^{-2}$ for the second term (II) in Eq. (13). This result is comparable to the ATTO 2015 case. The turbulent isoprene fluxes from other field studies are comparable in magnitude (e.g., Eerdekens et al. 2009).

- The third term (III), the turbulent transport of the numerator of I_s (e.g., Dlugi et al., 2014), is of order of $6 \cdot 10^{-5}\,ppb\,m\,s^{-1}$. This is in the upper range ($6 \cdot 10^{-6} - 6 \cdot 10^{-5}\,ppb\,m\,s^{-2}$) of the second term and within the lower part of the range of the first term. These findings will be discussed again when the storage term on the left side of Eq. (12) and R_{wi} are compared.

In the balance equation for the determination of the flux of isoprene (Eq. (12)) the first term on the right side (i) is composed of the vertical gradient and the variance of the vertical velocity component w.

- Taking results from the vertical gradients of isoprene at the ECHO site (e.g., Schaub, 2007; Ammann et al., 2004), the gradients vary in the range $0.01 - 0.25\, ppb\, m^{-1}$ while the average variance of w is about $0.25\, m^2\, s^{-2}$.
  This results in $2.5 \cdot 10^{-3} - 6.2 \cdot 10^{-2}\, ppb\, m\, s^{-2}$ for this term (i) commonly named *production of the isoprene* flux when there is a momentum flux in a flow field with a mean isoprene gradient. This movement across a vertical gradient of c_i is related to fluctuations in w as well as in c_i.

- The second term on the right (ii) relates the correlation between isoprene and vertical potential temperature to convective up- or downdrafts. For $\theta_v > T(K)$ the covariance varies between $0.02\, ppb\, K$ and $0.2\, ppb\, K$ (Dlugi et al., 2010). The quotient (g/θ_{v0}) is on average $(9.8/295)\, K\, m\, s^{-2}$. Therefore, the second term (ii) on the right side of Eq. (12) is in the range $6 \cdot 10^{-4} - 6.6 \cdot 10^{-3}\, ppb\, m\, s^{-2}$. For these conditions, term one (i) is larger than or equal to term two (ii).

- The third (iii) and the fourth (iv) terms on the right side of Eq. (12) cannot be calculated directly, because the corresponding measurements during ECHO 2003 and ATTO 2015 were performed only at one height, and, therefore, a vertical profile for the turbulent diffusion term of the flux is only available from the ECHO experiment on some days (see section 3.3), as also described by Dlugi et al. (2010, 2014). In addition, high frequency pressure fluctuations are not measured directly. Both terms can only be estimated based on measurements of the transport of heat, humidity, and CO_2 from studies on other days at the ECHO site (Section 3.3). The turbulent transport term (iii) itself is calculated from measurements (ECHO) for a height interval between 42 m and 28 m (with the main measuring height at $z_R = 37\, m$ (see Section 2.1)) and is of the order of $10^{-4} ppb\, m^2\, s^{-2}$. Compared to the turbulent transports of the heat flux and the turbulent kinetic energy from ECHO 2003 and other studies (e.g., Raupach, 1988; Raupach et al.,1996), the vertical gradient of the turbulent transport of isoprene is estimated to be of the order of $3 \cdot 10^{-6}\, to\, 10^{-5}\, ppb\, m\, s^{-2}$. This is significantly smaller than the first and second term of Eq. (12).

- The term (iv) is the most complicated to estimate. It redistributes c_i' within a volume and may be replaced by $1/\overline{\rho} \times \overline{p'(\partial c'/\partial z)}$ if – as commonly done – $\overline{p'c_i'}$ is assumed to be zero (e.g., Wyngaard, 1982). There are no experimental data available justifying such assumption. Therefore, problems exist quantifying this term by its theoretical derivation and the assumptions made to simplify the original term (e.g., Stull, 1988, Sorbjan, 1989) as well as by the experimental difficulties related to determine reliable values of p'. Here, two different approaches are applied to estimate the magnitude of this term. The first applies measurements of $\partial c_i'/\partial z$ and combines them with data on p' from literature.

  Different measurements of p' in canopies (e.g., Launder, 1978; Wyngaard, 1982; Shaw et al., 1990) showed that pressure fluctuations between about $0.1 - 15\,Pa$ are detected compared to mean values $\overline{p} \approx 1000\,hPa$. The mixing ratio fluctuations, c_i', are in the range of about $0.1\,ppb$ for ECHO 2003. For ATTO 2015 short time fluctuations of the isoprene mixing ratio larger by up to a factor of 15 are detected. This results for ECHO 2003 in values below $5 \cdot 10^{-4}\,ppb\,m\,s^{-1}$ if a maximum correlation coefficient $|r_{p\partial c}| = 0.6$ between p' and $\partial c_i'/\partial z$ as also given for momentum transfer for r_{uw} is assumed (Kaimal and Finnigan, 1994). For ECHO 2003 this term (iv) is estimated in the range of numerical values ($< 10^{-4}\,ppb\,m\,s^{-1}$) for the turbulent transport term (iii) (e.g., Stull, 1988; Sorbjan, 1989). For ATTO 2015, this term is larger, but $\leq 7 \cdot 10^{-4}\,ppb\,m\,s^{-1}$.

  The second approach applies an expansion by Launder (1978), using the Poisson equation for $1/\overline{\rho} \times \overline{p'(\partial c'/\partial z)}$, which relates this term to a sum of three terms with the dominant term given by $a_1 \cdot \left(\overline{w'c_i'}/\tau\right)$ with the closure constant in the range $2.5 \leq a_1 \leq 5.0$ (Lang and Bradley, 1983). Here the time scale τ is used according to the mixing length concept evaluated by Poggi et al. (2004) and applied by Cava et al. (2006) for measuring heights $z/h_c > 0.75$ with $a_1 = 2.9$. This approach results in a range of 10^{-3} to $5 \cdot 10^{-3} ppb\,m\,s^{-1}$ and is up to one order of magnitude larger than the result obtained by the first approach.

- The dissipation term ε_{wc} (vi) can be estimated according to Stull (1988) from the covariance of gradients of w' and c' times the sum of kinematic molecular diffusivities. This results in $\varepsilon_{wc} \leq 6 \cdot 10^{-8} ppb\,m\,s^{-1}$ for the data sets applied by Dlugi et al. (2014). Therefore, this term is smaller than the other terms in the air volume above canopy top.

Atmos. Chem. Phys. Discuss., https://doi.org/10.5194/acp-2018-1325
Manuscript under review for journal Atmos. Chem. Phys.
Discussion started: 17 May 2019

The storage term S_{wi} is directly calculated from field data (Fig. 2). As a result, the storage term S_{wi} on the left side of Eq. (12) is comparable in magnitude to R_{wi} and the residuum RF composed of all terms (i) - (vi) on the right side without R_{wi} (see Fig. 2).

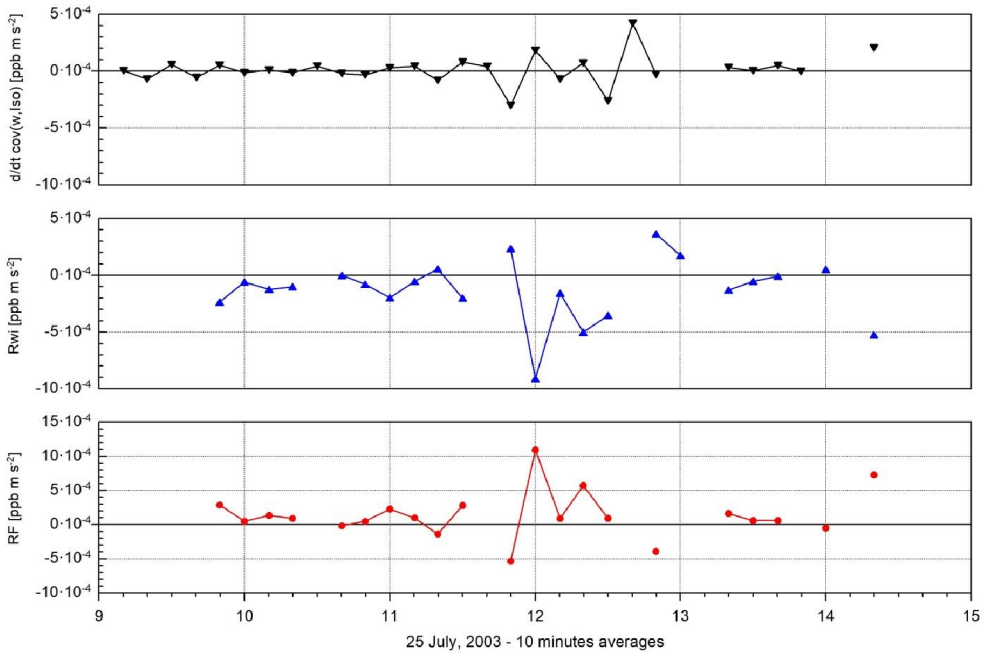

Fig. 2 The storage term of the balance of the flux, the chemical reaction term $\boldsymbol{R_{wi}}$, and the residuum, $\boldsymbol{RF}$, (see text) in Eq. (12) for the conditions during ECHO 2003 (25.07.2003) at height $\boldsymbol{z_R = 37\ m}$ at the main tower.

A net balance exists with $S_{wi} = RF + R_{wi}$ for the isoprene flux. Often S_{wi} is small compared to the other terms, which compensate each other. But for convective conditions during 25 July 2003, between 11 – 13 CET, S_{wi} becomes comparable in magnitude to the other terms (e.g., Dlugi et al., 2014). Therefore, even if advection with the mean flow is not discussed here, the influence of turbulent and convective transport and mixing expressed by term RF is comparable to R_{wi} in magnitude. The role of term (vi) remains uncertain as long as an evaluation of the Launder (1978) expansion for isoprene is missing, as it was done for heat and moisture by Lang and Bradley (1983).

Note that Eq. (12) describes the variability with time of the isoprene flux, $\overline{w'c_i'}$. If we assume that S_{wi} is always smaller than other terms – e.g., neglect some larger values in Fig. 2 and use $S_{wi} \equiv 0$ – a diagnostic equation can be formulated as an estimate for $\overline{w'c_i'}$.

$$\overline{w'c_i'} = \frac{1}{k_{ij} \times \overline{c_j}} RF - \frac{\overline{c_i}}{\overline{c_j}} \times \overline{w'c_j'} - \frac{1}{\overline{c_j}} \times \overline{w'c_i'c_j'} \,. \tag{14}$$

As mentioned above the flux $\overline{w'c_j'}$ is often assumed to be zero. In this case the flux of isoprene would be determined by RF (= sum of four terms (i) - (iv)) and term (v) in Eq. (12) multiplied by $\tau_c = \left(k_{ij} \cdot \overline{c_j}\right)^{-1}$, the chemical time scale for this reaction (e.g., Patton et al., 2001; Finlayson-Pitts and Pitts Jr., 1986) if term (I) in Eq. (13) can be neglected as discussed above. Therefore, a direct relationship between $\overline{w'c_i'}$ and $\overline{c_i'c_j'}$ or even with I_s is not given by Eq. (12) or Eq. (14), but a relation with the turbulent transport of the covariance $(\overline{w'c_i'c_j'})$ or with the four terms in RF can be established by Eq. (14).

3.5. The Balance of the Segregation Intensity

A diagnostic balance equation for I_s was described and discussed by Dlugi et al. (2014). Their analysis is based on the balance equation of the covariance $\overline{c_i'c_j'}$ which is the numerator in Eq. (1) for I_s. A short summary of this concept is given in the following. This balance equation reads:

$$S_{cov} = \frac{\partial}{\partial t} \overline{c_i'c_j'} = -TPI_k - TPOH_k - A_{1k} - A_{2k} - TT_k - D + R_{ij} \tag{15}$$

with the *residual term* RES (see Eq. (10) in Dlugi et al., 2014)

$$-RES = -TPI_k - TPOH_k - A_{1k} - A_{2k} - TT_k - D \tag{16}$$

S_{cov} is the storage term; TPI_k is the turbulent production by a turbulent flux of $isoprene$ in a spatially inhomogeneous field of OH. $TPOH_k$ is the turbulent production by a turbulent flux of OH in a spatially inhomogeneous field of isoprene. As mentioned above, the turbulent fluxes of OH ($\overline{w'OH'}$, along the z - coordinate) are solely caused by the influence of chemical sources P_{OH} and sinks L_{OH} of OH (Dlugi et al., 2010; 2014), because OH has a chemical *life-time* $\tau_{OH} < 1\,s$ and is not transported above a spatial scale of one meter or so in the atmosphere. A_{1k} is the advection of covariance by the influence of the divergence of the flow field; A_{2k} is the advection of covariance with the mean flow; TT_k is the turbulent transport of the covariance $\overline{c_i'c_j'}$; D is the molecular diffusion term and R_{ij} the chemical reaction term.

The magnitude of

- D is generally below $10^{-8}\ ppb^2\ s^{-1}$ and
- S_{cov} is found experimentally to be below $6 \cdot 10^{-8} ppb^2\ s^{-1}$,
- while all other terms are in the range $10^{-6} ppb\ s^{-1} \leq terms \leq 4 \cdot 10^{-4} ppb\ s^{-1}$ (see also Table 3 in Dlugi et al., 2014).

For the reaction (Eq. (4)) $(ISO + OH)$ during the ECHO 2003 and ATTO 2015 field studies the storage S_{cov} on the left side of Eq. (15) is significantly smaller than the other terms. Therefore, stationarity conditions ($S_{cov} = 0$) can be applied and Eq. (15) reads

$$RES = R_{ij} \tag{17}$$

with $$R_{ij} = -k_{ij} \times \left[\underbrace{\left(\overline{c_i' c_j'}\right) \times \left(\overline{c_i} + \overline{c_j}\right)}_{a} + \underbrace{\overline{c_i} \times \overline{c_j'^2}}_{b} + \underbrace{\overline{c_j} \times \overline{c_i'^2}}_{c} + \underbrace{\overline{c_i' c_i' c_j'}}_{d} + \underbrace{\overline{c_i' c_j' c_j'}}_{e} \right] \tag{18}$$

Note that the covariance in Eq. (1) is given in the first term of Eq. (18), and, therefore a diagnostic relation for $\overline{c_i' c_j'}$ (outgoing from the balance of the covariance) can be formulated based on R_{ij}.

Dlugi et al. (2014) solved Eq. (18) for $\overline{c_i' c_j'}$ and combined this formula with Eq. (17). This results in Eq. (20), if for $\overline{c_i} \approx 1\ ppb\ (ISO)$ and $\overline{c_j} \approx 10^{-4}\ ppb\ (OH)$, also the relation $\overline{c_i} \gg \overline{c_j}$ is considered with

$$C_{ij} = \underbrace{\overline{c_i} \times \overline{c_j'^2}}_{b} + \underbrace{\overline{c_i' c_i' c_j'}}_{d} + \underbrace{\overline{c_i' c_j' c_j'}}_{e} \tag{19}$$

$$-\overline{c_i' c_j'} = \frac{1}{k_{ij} \cdot \overline{c_i}} \times \left(RES + k_{ij} \times C_{ij}\right) - \frac{\overline{c_j}}{\overline{c_i}} \times \overline{c_i'^2} = RE + \frac{C_{ij}}{\overline{c_i}} - \frac{\overline{c_j}}{\overline{c_i}} \times \overline{c_i'^2} \tag{20}$$

The same *order of magnitude estimation* as performed for the balances of the variance and the flux shows that only the second term (d) in C_{ij} (Eq. (19)) contributes to the covariance (Dlugi et al., 2014). Finally if Eq. (20) is divided by $\overline{c_i} \times \overline{c_j}$ a diagnostic equation for I_s (see Eq. (1)) is obtained:

$$-I_s = \underbrace{\frac{RES}{k_{ij} \times \overline{c_i} \times \left(\overline{c_i} \times \overline{c_j}\right)}}_{I} + \underbrace{\frac{\overline{c_i' c_i' c_j'}}{\overline{c_i} \times \left(\overline{c_i} \times \overline{c_j}\right)}}_{II} - \underbrace{\frac{\overline{c_i'^2}}{\overline{c_i}^2}}_{III} = RE_{is} + CH_{is} - nvar(ISO)_{is} \tag{21}$$

Here only the numerator of the first term (I) in Eq. (21) is unknown, if measurements at one height could be performed to study segregation as it was done during ECHO 2003 and ATTO 2015. As described by Dlugi et al. (2014) (their Table 3) most terms composing RES can be estimated by their order of magnitude for ECHO 2003. All other terms can be directly calculated from measurements. Note that both terms, CH_{is} and the normalized variance of isoprene $nvar(ISO)_{is}$, originate from R_{ij} (Eq. (18)). The (normalized) variance of isoprene was shown to correlate well with I_s by experimental data analysis (Dlugi et al., 2014) and

modelling studies (e.g., Patton et al., 2001; Vinuesa and Vilà-Guerau de Arellano, 2005; Ouwersloot et al., 2011) and was therefore separated from all other terms of the chemical term that are contained in CH_{is}. This is because the OH mixing ratios and variances are small compared to the isoprene mixing ratios and variances. The same analysis as for ECHO 2003 was applied to ATTO 2015 data.

At first we compare terms of Eq. (18) for ATTO 2015. The calculation of all terms $(a - e)$ of R_{ij} (Eq. (18)) shows that terms a and c are dominant (Fig. 3) for ATTO 2015 as well as for ECHO 2003 (see Fig. 12 in Dlugi et al. (2014)). Term a serves to formulate the left side of Eq. (20). Term c originates from the third term on the right side of Eq. (18), and, finally becomes $nvar(ISO)_{is}$ in Eq. (21).

Although term c is positive definite, other terms like term a or d in Eq. (18) are not. Therefore R_{ij} also becomes negative (Fig. 3). The relation between term c of R_{ij} and R_{ij} itself for both experiments is expressed by the presentation in Fig. 4. The error bars in Fig. 6 and Fig. 7 for ECHO 2003 are given by the uncertainties of the covariance in I_s (Eq. 1) and R_{ij} as well as higher moments in σ_i^2 and CH_{is}, if the time delay between time series of ISO and OH is varied by up to $\pm 0.2\ s$. This time shift estimates the influence of wind vector variation inside the sampling volume, as discussed by Dlugi et al (2014).

Atmos. Chem. Phys. Discuss., https://doi.org/10.5194/acp-2018-1325
Manuscript under review for journal Atmos. Chem. Phys.
Discussion started: 17 May 2019

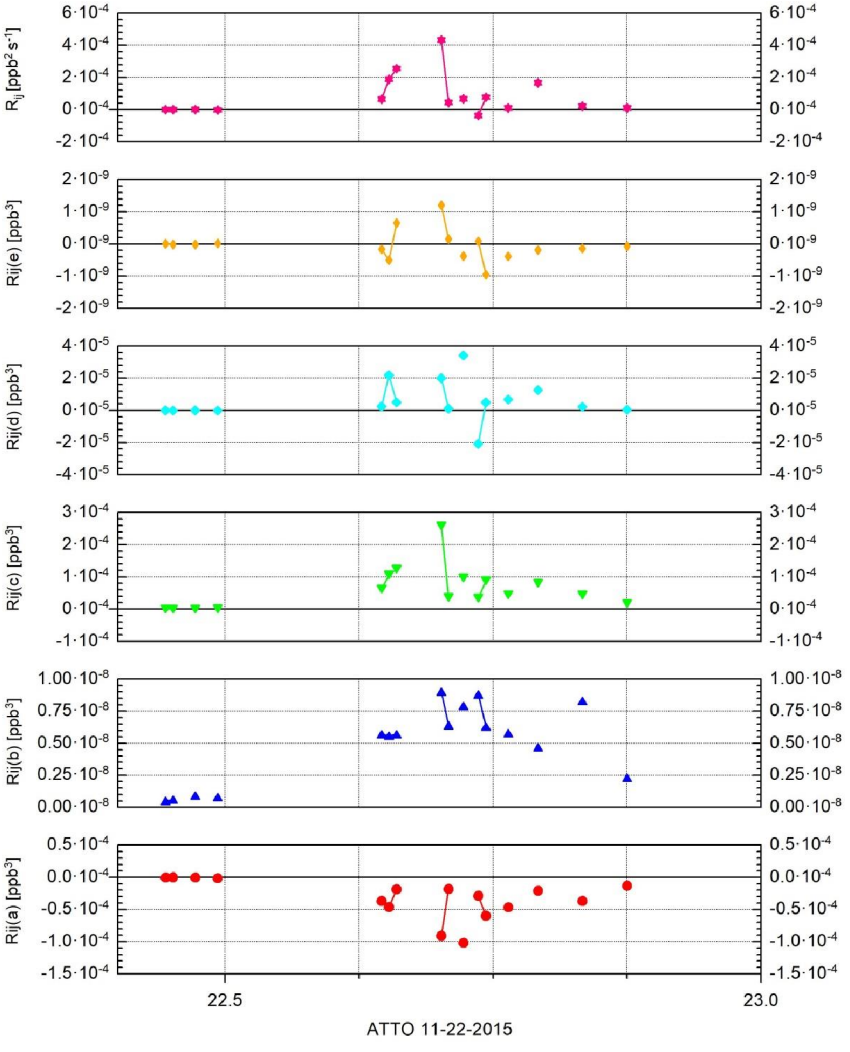

Fig. 3 The five terms of (Eq. (18)) and $\boldsymbol{R_{ij}}$ for ATTO on 22 November 2015.

Atmos. Chem. Phys. Discuss., https://doi.org/10.5194/acp-2018-1325
Manuscript under review for journal Atmos. Chem. Phys.
Discussion started: 17 May 2019

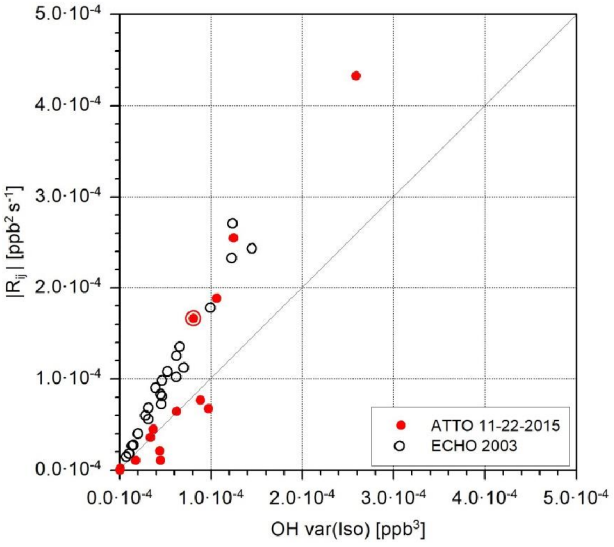

Fig. 4 The magnitude of $\boldsymbol{R_{ij}}$ as function of term $\boldsymbol{c}$ in Eq. (18) for ECHO (25 July 2003) and ATTO (22 November 2015). Data points before noon are clumped together near zero. (The circle gives the data point which deviates from the fit as described in the text).

The importance of the turbulent fluctuations of the isoprene mixing ratio for the magnitude of I_s, as pointed out by Patton et al. (2001) and Ouwersloot et al. (2011) from their modelling studies, is also proven by these experimental findings, as the reaction term can be well described by $(OH \times var(ISO))$ (Fig. 4). For $|R_{ij}| \leq 10^{-4} ppb^2\, s^{-1}$ the ECHO 2003 data are given by $|R_{ij}| \approx 2.15\,(OH \times var(ISO)) \approx k_{ij}\,(OH \times var(ISO))$, while the ATTO 2015 data follow $|R_{ij}| \approx 0.74\,(OH \times var(ISO))$ with the exception of one data point (circled, Fig. 4). The deviation of the ATTO results from those for ECHO is unknown up to now.

The time behavior of all terms in Eq. (21) for the situation during 22 November 2015 at the ATTO tower is given in Fig. 5. For comparison, the same four terms for the ECHO 2003 case study are shown in Fig. 6 as given originally by Dlugi et al. (2014).

Atmos. Chem. Phys. Discuss., https://doi.org/10.5194/acp-2018-1325
Manuscript under review for journal Atmos. Chem. Phys.
Discussion started: 17 May 2019

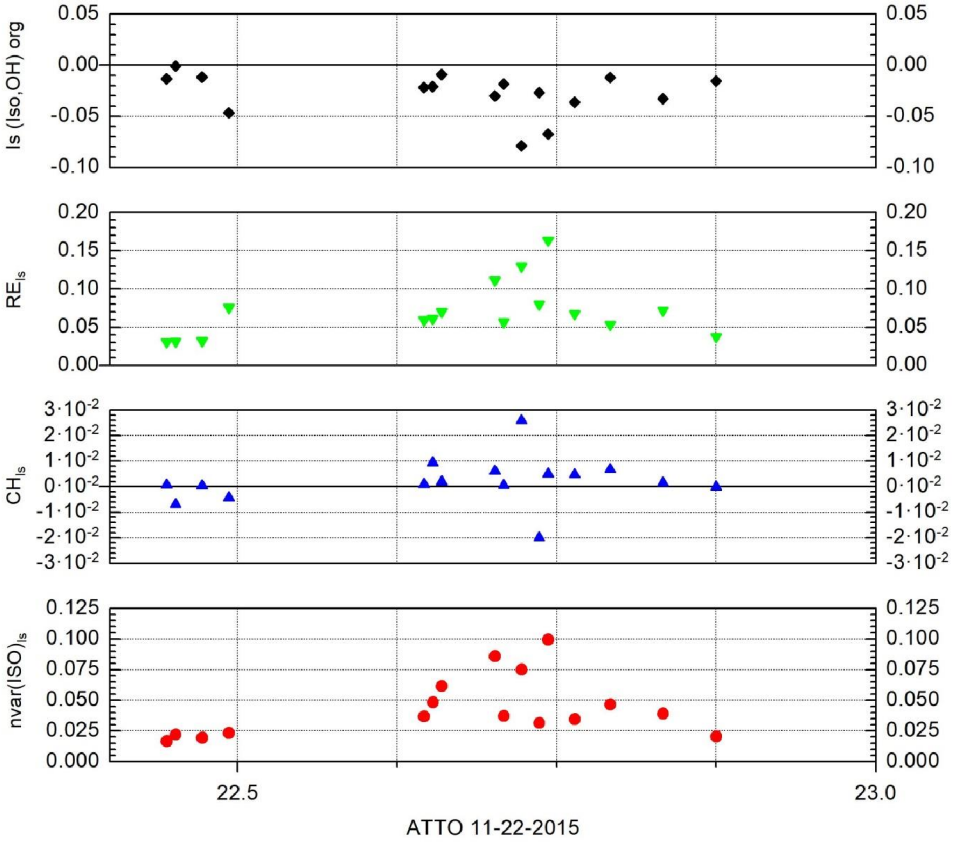

Fig. 5 The four terms of Eq. (21) for ATTO on 22 November, 2015 as function of time. (Note that the calculations of the third moments in Eq. (18) – Eq. (21) are performed in a way that only third order terms are selected which are above 2σ of the minimum value found in the data set.)

Atmos. Chem. Phys. Discuss., https://doi.org/10.5194/acp-2018-1325
Manuscript under review for journal Atmos. Chem. Phys.
Discussion started: 17 May 2019

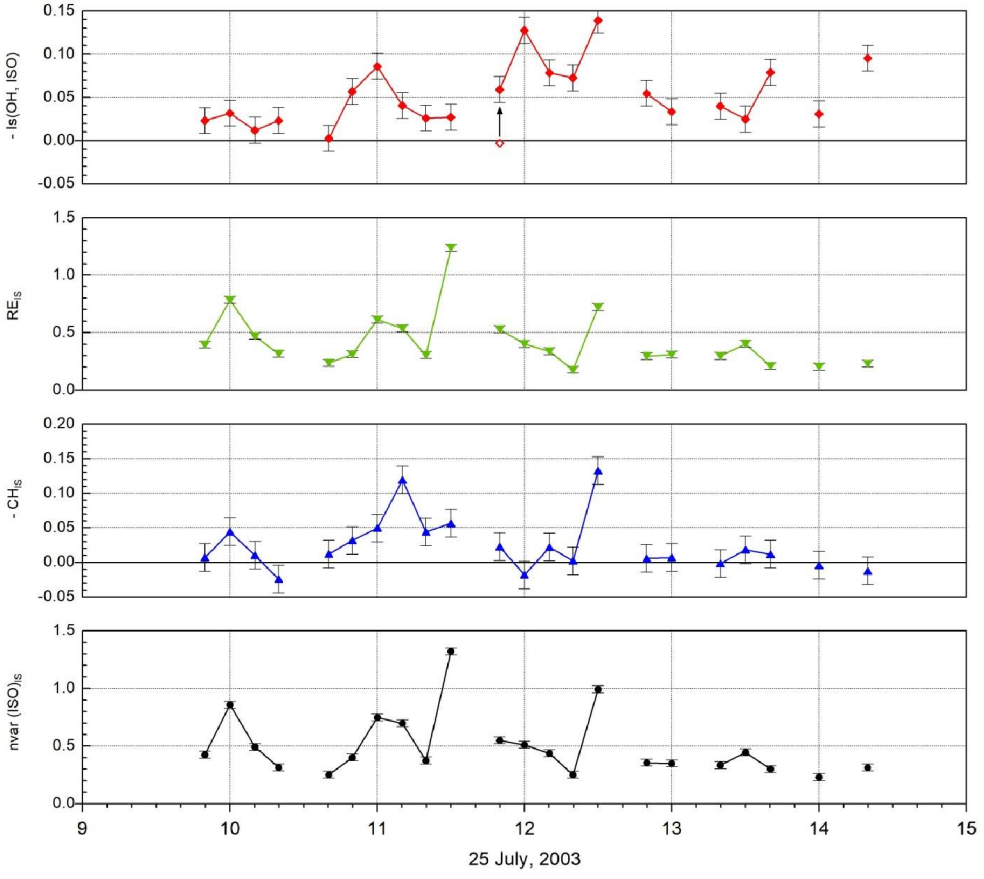

Fig. 6 The four terms of Eq. (21) for ECHO on 25 July, 2003 as function of time (adapted from the original presentation in Dlugi et al. 2014).

Atmos. Chem. Phys. Discuss., https://doi.org/10.5194/acp-2018-1325
Manuscript under review for journal Atmos. Chem. Phys.
Discussion started: 17 May 2019

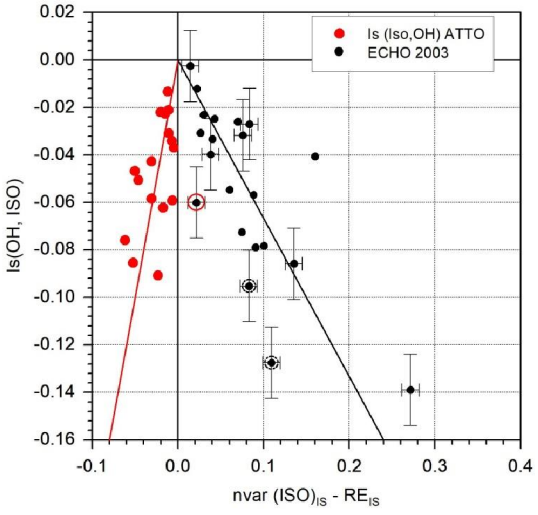

Fig. 7 The segregation intensity $\boldsymbol{I_s}$ as function of the difference $\boldsymbol{nvar(ISO)_{is} - RE_{is}}$ according Eq. (21) for the ECHO and the ATTO cases. (Note that the calculations of the third moments in Eq. (18) – Eq. (21) are performed in a way that only third order terms are selected which are above $\boldsymbol{2\sigma}$ of the minimum value found in the data set.) The circles around some ECHO 2003 data are explained in the text.

Although the magnitudes of $nvar(ISO)_{is}$, and therefore RE_{is} - but also CH_{is} – differ between the two studies by about an order of magnitude (Fig. 5, 6), the segregation intensities, I_s, some meters above the canopy top are comparable in magnitude with $|I_{s,ATTO}| \leq |I_{s,ECHO}|$. In both studies, CH_{is} is significantly smaller than $nvar(ISO)_{is}$ and RE_{is}, which are both of comparable magnitude. Therefore, $I_s \sim (nvar(ISO)_{is} - RE_{is})$ in Fig. 7. The three marked points (Fig. 7) for the ECHO 2003 case belong to two periodes of convective conditions (black circles) and one case where a correction was applied based on the analysis of the ogive for $\overline{c_i' c_j'}$ (red circle) as discussed in more detail by Dlugi et al. (2014) in their sections 5.3.4 and 4.2.4.

RE_{is} is the residuum determined by the other three terms in Eq. (21). None of these terms is near zero for ECHO 2003 (Fig. 6) as well as ATTO 2015 (Fig. 5). We find $nvar(ISO)_{is} > RE_{is}$ for ECHO 2003 which proves $CH_{is} \neq 0$ with an average value of $nvar(ISO)_{is} \approx 0.42$. For $I_s = -0.16$ (extrapolated from the ECHO 2003 data in Fig. 7) one obtains a mean value for $nvar(ISO)_{is} - RE_{is} = 0.24$, which results in mean values for $RE_{is} \approx 0.18$ and $CH_{is} \approx 0.08$ according to Eq. (21) for the ECHO 2003 case. But some data points for ECHO 2003 in Fig. 7 (circles around data points) fulfill the conditions $nvar(ISO)_{is} - RE_{is} < I_s$, which requires not only $CH_{is} < 0$ but even $|nvar(ISO)_{is}| < |RE_{is}|$ as discussed by Dlugi et al. (2014). The term CH_{is} - e.g., the triple moment in term (d) (Eq. (19)) - is either negative or positive (Fig. 5, 6).

For this ATTO case the term RE_{is} is always larger than $nvar(ISO)_{is}$. I_s is therefore dominated by this residual term (Fig. 5, 6) which describes the interactions between the turbulent flow field with the fields of both scalars.

Note that R_{ij} (eq. (18); Fig. 8) increases with increasing variance of the reactants. As mixing ratios and variances of isoprene are much larger than those of OH, the standard deviation of isoprene ($\sigma_i = \overline{(c_i'^2)}^{1/2} = std(ISO)$) is a main driver in the chemical terms, and, therefore, also for I_s (Eq. (3)) with a correlation coefficient $R = 0.91$ for ECHO 2003 and $R = 0.79$ for ATTO 2015 (Fig. 8). This reflects the important influence of this term *c* of Eq. (18) and of σ_i in Eq. (3) (Fig. 8). But the influences of turbulent transport and mixing in term RES respectively RE_{is} may even exceed the magnitude of $nvar(ISO)_{is}$ (Fig. 7). I_s, therefore, becomes controlled by chemical as well as dynamic and mixing processes enhancing the variances of the reactants, respectively σ_i (and / or σ_j). In addition the variation of the surface source strenghth E_{oi} in space and time influences σ_i.

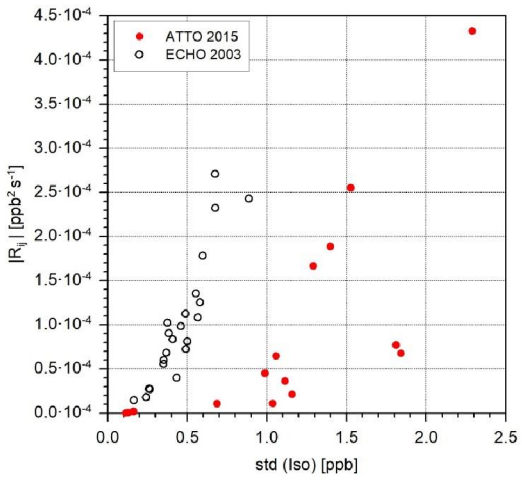

Fig. 8 $\boldsymbol{R_{ij}}$ (see Eq. (18)) as function of the isoprene standard deviation for ECHO 2003 and ATTO 2015.

The quantities σ_i, σ_j and the correlation coefficient r_{ij} from the numerator in Eq. (3) define the magnitude of I_s. The correlation coefficient $r_{ij} = r(OH, ISO)$ from the field increases for both cases non-linearely with increasing I_s (Fig. 9). All values of r_{ij} from experiments are found below a line $|r_{ij}| = 2.5 \cdot |I_s|$ (for $-0.4 \leq I_s \leq 0$) and are smaller than $r_{ij} = -0.6$. Note that this relation is very similar for ATTO 2015 and ECHO 2003 (Fig. 9).

Atmos. Chem. Phys. Discuss., https://doi.org/10.5194/acp-2018-1325
Manuscript under review for journal Atmos. Chem. Phys.
Discussion started: 17 May 2019

Dlugi et al. (2010; 2014) discussed the influence of instrumental (white) noise on r_{ij}. The contribution of noise to the isoprene mixing ratio is small (e.g., Spirig et al., 2005) and only influences σ_i by less than 5% for ECHO 2003 and by less than 1% for ATTO 2015. In contrast, the signal to noise ratio of the measured mixing ratios of the hydroxyl radical is sometimes only 3.

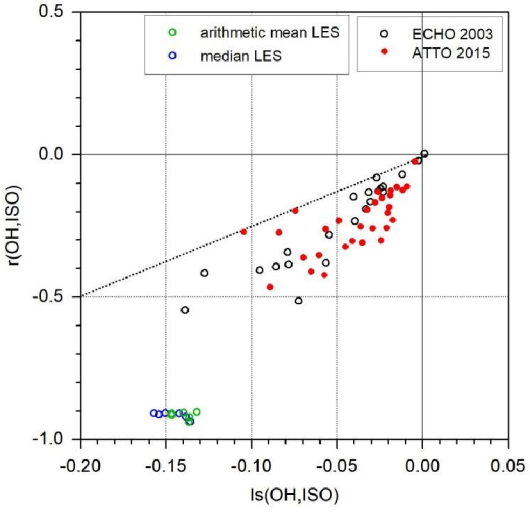

Fig. 9 The correlation coefficient in Eq. (3) between $\boldsymbol{OH}$ and isoprene for ECHO 2003 and ATTO 2015 and from the LES model for a layer of 10 m to 30 m above the surface (Ouwersloot et al., 2011).

The σ_j is influenced in such case by the impact of noise on the variance and becomes larger by up to 15%. Therefore, if the standard deviation σ_j increases by up to 15%, r_{ij} in Eq. (3) becomes smaller by this magnitude as compensation. If this estimate is applied to all data in Fig. 9, the largest correlation coefficient from ECHO 2003 would be about $r_{ij} = -0.65$. This is still below the theoretically applied $r_{ij} \geq -0.7$ for modelling studies (e.g., Table 3). Ouwersloot et al. (2011) calculated r_{ij} explicitly in their LES model and obtained medians and arithmetic means of about $r_{ij} \approx -0.9$ (Fig. 9) for the lowest layers between 10 m and 30 m above the surface. A significant difference exists between the correlation coefficients from field measurenents and modelling. On the other hand the covariances (in Eq. (2)) and I_s (in Eq. (1)) are rarely modified by instrumental noise as shown for the background signals of the PTR-MS instrument and the LIF for the ECHO 2003 study. This means that these signals have characteristics near white noise and, therefore, are not correlated (e.g., Wu et al., 2007; Sachs and Hedderich, 2006).

4. Variability of Segregation Intensity

4.1. Relation between Segregation Intensity and Surface Flux

In addition to the results discussed by Dlugi et al. (2010, 2014), the segregation intensity can be presented in terms of Eq. (6) to establish an empirical relationship to the turbulent flux of isoprene. As mentioned before, such a direct proportionality between I_s and $\overline{w'c_i'}$, is stated by Kaser et al. (2015) and others. In Section 3 (3.3; 3.4) we discussed which prognostic and diagnostic relations exist to establish such a relation.

The analysis of the data from ECHO 2003 and ATTO 2015 related to Eq. (6) yields the results given in Fig. 10 for all isoprene fluxes. During ECHO 2003, the influence of convective transport by clouds was occasionally observed and caused significant up- and downdrafts at the main tower only 7 m above canopy top (Dlugi et al., 2014). The downward motion was observed also for sensible and latent heat and resulted in situations with net downward transport of isoprene (note that a covariance $\overline{w'\alpha'}$ is always composed of positive (upward) and negative (downward) values of vertical wind velocity w and the corresponding values of α during the averaging time T). The downward (negative values of w) motion was observed to dominate in the range below $10^{-2}Hz$ for some averaging periods $T = 600\ s$. This caused the cumulative (flux) covariance (the *ogives*) to be negative in this frequency range. For higher frequencies the ogives were positive, which can be related to the influence of the emission flux. Thus $\overline{w'c_i'} = 0$ (see Fig. 10) results from spectral compensation of upward and downward motion (see also Fig. 12 in Dlugi at al. 2014 and the discussion on Fig. 7).

If only the upward-directed (positive) turbulent isoprene flux values from measurements near canopy top are considered (Fig. 11), the statistical correlation with I_s improves. Compared to the complete results in Fig. 10 for ECHO 2003, the coefficient of determination, Eta^2_{adj}, increases from $Eta^2_{adj} \approx 0.40$ to $Eta^2_{adj} \approx 0.56$, also together with the correlation coefficient. But still about 44% of the variance is not accounted for by the linear regression in Fig. 11 (e.g., Sachs and Hedderich, 2006). This result cannot be improved even if the other terms in Eq. (6) would perfectly correlate ($R = 1; Eta^2_{adj} = 1$) with I_s. A comparable result is obtained for on 22 November during ATTO 2015.

A negative correlation between I_s and the measured isoprene flux is given in Fig. 10 or Fig. 11 and is also described by Kaser et al. (2015), but with $Eta^2_{adj} = 0.1156$ and a correlation coefficient $|R| = 0.34$. Therefore, less than 12% of the variance of these data from a flight

track in the ABL for the relation between I_s and $\overline{w'c_i'}$ is described by this regression (see Fig. S5 in Kaser et al., 2015).

The ECHO 2003 and ATTO 2015 measurements were performed near the canopy top ($z/z_i \cong 0.03$) (see: Section 2.), while the NOMADSS 2013 results are calculated from aircraft measurements at $z/z_i \approx 0.4$ with z_i = ABL height. We applied the convective boundary layer (CBL) scaling for fluxes (e.g., Moeng and Wyngaard, 1984; Wyngaard and Brost, 1985; Moeng and Sullivan, 1994; Hess, 1992; Patton et al., 2003) to a measured mean for the isoprene flux of about $0.1\, ppb\, m\, s^{-1}$ for this flight track (see Fig. S5 (supplement), Kaser et al., 2015) and estimated a surface flux in the range of $1 - 1.3\, ppb\, m\, s^{-1}$. This result agrees to average isoprene fluxes given by Su et al. (2015) (in their Fig. S5) determined in the same region for conditions around noon in June 2013.

To understand both findings we compare them with the results of the first studies on balances of second moments of scalars and their relation to the mean fields of related quantities in the ABL as presented by Stull (1988) based on research done by Lenschow et al. (1980), André et al. (1978), Deardorff (1974), Caughey and Palmer (1979) and Zhou et al. (1985) for virtual potential temperature θ_v and by Deardorff (1974) and Lenschow et al. (1980) for specific humidity q. These authors performed their analysis on data of day 33 of the Wangara – experiment 1967. Further references to analysis of this kind are summarized and discussed - for example - in Haugen (1973), Sorbjan (1989) or Garrett (1992).

The analysis of the balances of variances ($\overline{\theta_v'^2}$ or $\overline{q'^2}$) show that the gradient *production term* GP_{var} (see Eq. (11)) has maximum values at the surface. The magnitude of GP_{var} decreases with increasing height with minima around $z/z_i \approx 0.2$ for $\overline{q'^2}$ and in the interval $0.5 \leq z/z_i \leq 0.8$ for $\overline{\theta_v'^2}$ during the early afternoon. As the contribution of the production term GP_{var} decreases with increasing height, the contributions of other terms in the budget increases. Therefore, a relation between term GP_{var} respectively the turbulent flux $\overline{w'c_i'}$ in Eq. (11a) and $\overline{c_i'^2}$ is only established near the Earth surface where a certain correlation exists, but with a correlation coefficient $|R| < 0.77$ between I_s and $\overline{w'c_i'}$ (Fig. 10, Fig. 11).

Atmos. Chem. Phys. Discuss., https://doi.org/10.5194/acp-2018-1325
Manuscript under review for journal Atmos. Chem. Phys.
Discussion started: 17 May 2019

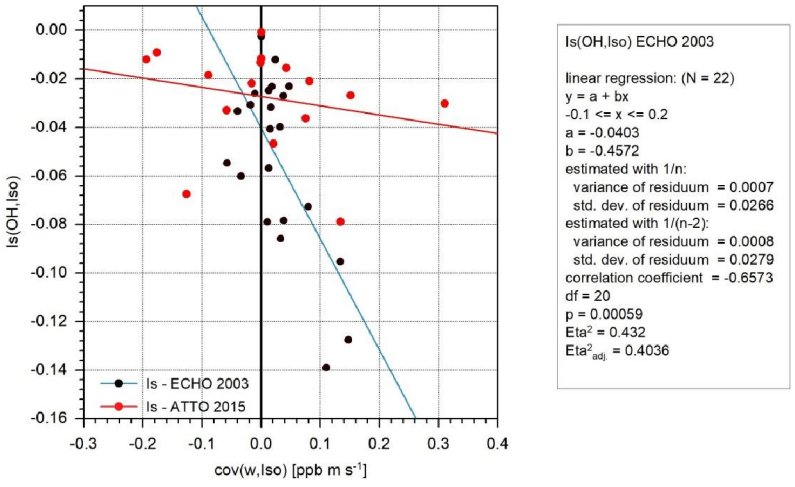

Fig. 10 The segregation intensity, $\boldsymbol{I_s}$, (ECHO: 25 July, 2003 and ATTO: 22 November, 2015) as function of the turbulent isoprene flux above canopy top with the influence of net downward and upward motion. (Linear regression for ATTO 2015: $\boldsymbol{N = 16}$; $\boldsymbol{a = -0.0273}$; $\boldsymbol{b = -0.038}$; correlation coefficient = $\boldsymbol{-0.2297}$)

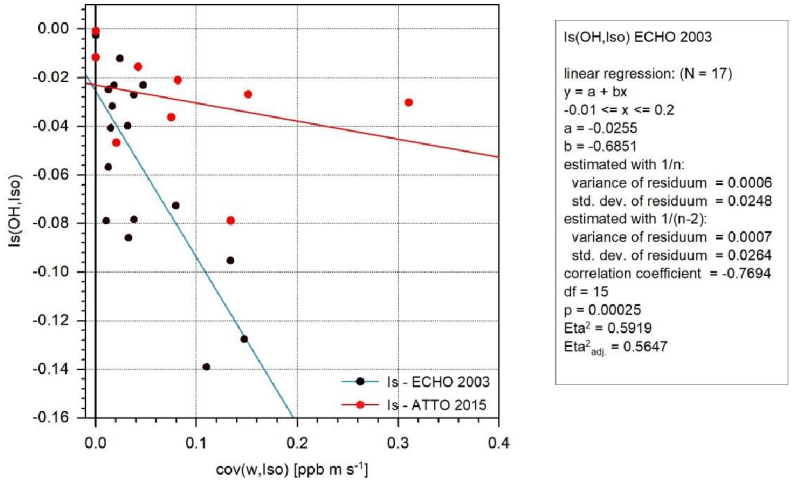

Fig. 11 The segregation intensity, $\boldsymbol{I_s}$, (ECHO: 25 July, 2003 and ATTO: 22 November, 2015) as function of only the upward directed turbulent fluxes of isoprene. (Linear regression for ATTO 2015: $\boldsymbol{N = 9}$; $\boldsymbol{a = -0.023}$; $\boldsymbol{b = -0.0742}$; correlation coefficient = $\boldsymbol{-0.3196}$)

With increasing height in the ABL, $\overline{c_i'^2}$ (respectively $\sigma_i = \left(\overline{c_i'^2}\right)^{1/2}$) is also determined by the growing influence of other terms (and even vertical advection), so that the correlation between I_s and the flux $\overline{w'c_i'}$ in GP_{var} decreases significantly. This agrees with the result obtained by Kaser et al. (2015) which becomes different for fluxes measured near the top of a forest (Fig. 10 and Fig. 11) in ECHO 2003 or ATTO 2015. As discussed in Section 3.4 the near surface isoprene flux (Eq. (14)) is not primarily determined by the convective (heat) flux but by the production term (i) in Eq. (12) and by the chemical reaction term R_{wi} (Eq. (13), Fig. 2).

Although our CBL scaling - applied to the fluxes given for NOMADSS for the flight level at $z/z_i \approx 0.4$ down to the surface - yields reliable results, the fluxes of isoprene and sensible heat given by Kaser et al. (2015) at $z/z_i \approx 0.4$ are not significantly correlated to each other. Note that even in the NOMADSS 2013 case (flight RF13), where free convective conditions in the ABL around noon may exist (e.g., Su et al., 2015), the correlation between the fluxes of sensible heat and isoprene ($Eta_{adj}^2 = 0.1781$) at the mean flight level $z/z_i \approx 0.4$ is weak (Fig. S6 in Kaser et al., 2015), as 82% of the variance is not explained by the correlation (e.g., Sachs and Hedderich, 2006).

The NOMADSS sensible heat flux data show dominant up- and downdrafts – as it should be observed in a CBL – with most results in a range $-0.03 < \overline{w'T'} < 0.13\ K\ m\ s^{-1}$. Note that some larger positive and negative fluxes are "*excluded from fit*" (Fig. S6 in Kaser et al., 2015). If we applied the convective scaling also to estimate the mean sensible heat flux at the surface, values around $H_s \approx 0.1\ K\ ms^{-1}$ are obtained, again also in agreement with results reported by Su et al. (2015).

In addition, other observations in the CBL show that at $z/z_i \approx 0.4$ the amount of downward (negative) fluxes are between 10% to 40% (e.g., Stull, 1988; Patton et al., 2003). Su et al. (2015) assume a relation for heat transport between entrainment flux and surface flux of 20% as a mean value for the CBL. If a higher correlation exists between both fluxes at the surface, this relation is reduced by downdrafts of sensible heat with increasing height in the CBL. Therefore a correlation between I_s and $\overline{w'c_i'}$, as found near the surface, vanishes with increasing height in the ABL, consistent with other experimental findings and results from modelling.

4.2. Is there an Upper Limit for the Segregation Intensity in the *OH – Isoprene* Reaction?

4.2.1 The Relation between Covariance and Product of the Means

Most results on segregation for atmospheric conditions are derived from modelling. A selection of such results for reaction Eq. (4) and a comparison with experimental findings is given in Table 3. Maximum values for I_s near the Earth surface, respectively near canopy top ($z_R \approx h_c$ and $z_R/z_i < 0.05$), are in the range $-0.27 \leq I_s \leq -0.02$, if results from experiments and LES models are considered.

Kaser et al. (2015) report on a range of I_s from flight RF13 of $-0.17 \leq I_s \leq -0.09$ and for flight RF17 of $-0.19 \leq I_s \leq -0.085$ at a mean flight level z_F of about $z_F/z_i \approx 0.4$. They mention that "*during flight R17, local segregation was measured as large as* -0.3" and they relate the high values to "*surface heterogeneity larger than typical PBL scales*", e.g., to source areas of this size with higher isoprene emission fluxes.

Note that with their time resolution for OH measurements of $30\ s$ ($0.03\overline{3}\ Hz$) and the mean flight velocity of $100\ m\ s^{-1}$ they obtained one OH data point every $3\ km$, 17 data points for a $51\ km$ flight leg and 34 data points for a $102\ km$ leg. The spectral maximum of I_s is given for a time scale of about $730\ s$, which includes about 24 data points and corresponds to a root mean square of about 20%.

The surface heterogeneities in the emission rates, where high values in the order of $I_s \approx -0.3$ were determined by Kaser et al. (2015), are related to surface scales larger than z_i. For the flight RF13 and $z_i \approx 2200\ m$, spatial scales of the order of three to six times the value of z_i may cause such high values. But for such a flight leg of about $6.6\ km$ to $13.2\ km$ only about two to four (or five) data points from the OH instrument are available for the calculation of I_s, which results in a root mean square larger than 47%.

For comparison, the time resolution for the analysis of the data of OH and isoprene during ECHO 2003 and ATTO 2015 was $0.2\ Hz$ and $0.067\ Hz$, respectively, leading to 120 OH data points (respectively 40 data points) in the time intervals of $600\ s$, which were considered for the analysis by Dlugi et al. (2010) and Dlugi et al. (2014), respectively, and in this study for ATTO 2015. The root mean square error of these data sets is about 9.1% and 15.8%, respectively.

To introduce a higher time resolution, Kaser et al. (2015) extended the OH - spectra from about $0.03\ Hz$ to higher frequencies using spectra of O_3 - variance and covariance, $\overline{O_3'ISO'}$, as a surrogate of $\overline{OH'ISO'}$. This approach is not justified a priori, because the mixing ratios of OH and O_3 are not related to each other in a 1:1 relation.

Based on this modified data set, they present a wavelet analysis for the cross spectrum of the covariance $\overline{c_i'c_j'}$ for the wavelet scale $> 80\ s$ to show that I_s maxima occur at time scales between $500\ s$ to $1000\ s$. These time scales correspond to spatial scales of about $50\ km$ and $100\ km$, according to the mean flight velocity of $100\ m\ s^{-1}$.

Therefore, their statement, that "*an increase in isoprene flux*" – by such a strong surface source – "*should lead to an enhanced production of I_s as observed in the real data sets*" (Kaser et al., 2015), is not based on conclusive results, as also described in Section 4.1. As discussed above, this result is not surprising, because the statement supposes that the emission flux, E_{i0}, is directly related to $\overline{w'c_i'}$ at any height in the ABL and – in addition – that this isoprene flux significantly correlates with I_s. But this relation, $I_s \approx f(\overline{w'c_i'})$, can only exist near the surface if the variance (and therefore σ_i) is mainly controlled by the term GP_{var} in Eq. (9) and Eq. (11). At the flight level of $z_F/z_i \approx 0.4$, the low correlation found by Kaser et al. (2015) proves that this relation is no longer valid and other terms in the balance of the variance are of larger influence as described for heat and moisture from the analysis of earlier studies in Stull (1988).

Kaser et al. (2015) also suggest that the covariance $\overline{c_i'c_j'}$ in Eq. (1) is directly proportional to the product of mean mixing ratios, $\overline{c_i} \times \overline{c_j}$. The only data set showing such a relationship was presented by Dlugi et al. (2014) and is given in Fig. 12 together with an extended analysis of ECHO 2003, data from ATTO 2015, and the values modelled by LES for the lowest layer and inhomogeneous conditions (Ouwersloot et al., 2011). In addition, two data points from flight RF13 and RF17 are added from Kaser et al. (2015), which are estimated from their Table 1 and Table S2 (in their supplement). For RF13 and RF17, only the mean mixing ratio of the PTR-MS instrument measuring isoprene is used as reported in their Table S2. Therefore only mean values of the covariances can be calculated, but not their ranges as given for I_s in Table 3 (according to Table 1 of Kaser et al., 2015).

Atmos. Chem. Phys. Discuss., https://doi.org/10.5194/acp-2018-1325
Manuscript under review for journal Atmos. Chem. Phys.
Discussion started: 17 May 2019

Atmospheric Chemistry and Physics Discussions

Tab. 3 Overview of different terms of Eq. (1) from modelling (1 – 6) and experiments (7 - 9) for the reaction $ISO + OH$ (Sk = skewness; ν = frequency; c_i = mixing ratio; h_c = canopy height; z_i = ABL – height; u_* = friction velocity)

	Authors	I_s	Da_c	$r_{ISO,OH}$	Spectral Range	Comments
1	Peterson and Holtslag (1999)	-0.27 (LES) -0.4 (1-D)	≈ 0.65	n.a.	n.a.	their Tab 2.6 and Chpt. 5 for: $z/z_i < 0.05$
2	Patton et al. (2001)	-0.175 (near h_c) (LES)	0.17	≥ -0.7	$4 \cdot 10^{-4} \leq \nu \leq 0.16\text{Hz}$	Sk_w << measured $Sk_{w,c}$ therefore r_{ij} (model) > r_{ij} (experiment)
3	Verver et al. (2000)	below – 0.1 below -0.02	≈ 0.18 ≈ 0.05	n.a.	n.a.	Morning hours and afternoon Diurnal cycle of Da_c and I_s
4	Vinuesa and Vilà-Guerau de Arellano (2005)	-0.17 -0.1 (LES)	≈ 0.6 ≈ 0.3 (LES)	≥ -0.75	n.a.	near $z/z_i \approx 0.1$ near $z/z_i \approx 0.05$
5	Ouwersloot et al. (2011)	-0.195 (max) (LES) -0.07 to -0.09 (LES)	about 0.2	> -0.7		Inhomogeneous isoprene emission; for homogeneous isoprene emission: r_{ij} increases with increasing R_{ij} (Eq.(1))
6	Kaser er al. (2015)	LES: -0.3 / -0.47 (a) -0.1 to < -0.3 (b)	about 0.4	≥ -0.7 (see (2.))	about $4 \cdot 10^{-4} \leq \nu \leq 0.1\text{Hz}$	(a) $z/z_i \approx 0.027$ near $z = h_c$ homogeneous / inhomogeneous emission (b) $z/z_i \approx 0.4$; homogeneous / inhomogeneous emission
7	Kaser er al. (2015)	-0.13; -0.09 to -0.17 -0.14; -0.085 to -0.195 max: -0.19 to -0.3	≈ 0.42 n.a.	estimate < -0.7	$4.5 \cdot 10^{-4} \leq \nu \leq 0.03\text{Hz}$ $8 \cdot 10^{-4} < \nu < 2 \cdot 10^{-3}\text{ Hz}$	mean and variation for flight track; variation for high ISO sources
8	This work: Based on data from Dlugi et al. (2010, 2014) from ECHO	-0.15 to -0.01 -0.21 to -0.02*	$0.01 < Da_{t_1} < 0.1$ $0.03 < Da_{t_2} < 0.3$	< -0.56 ≤ -0.65	$1.6 \cdot 10^{-3} \leq \nu \leq 0.2\text{Hz}$ $5 \cdot 10^{-4} \leq \nu \leq 0.2\text{Hz}$*	$\tau_{t1} = h_c/u_*$ (see 2.); $z/z_i \approx 0.03$; *spectral contributions below $1.6 \cdot 10^{-3}$ Hz contribute up to 23% to I_s ! τ_{t2} from Lagrangian diffusion with $\tau_{t_2} \approx (3.0\ to\ 4.0)\tau_{t_1}$ (see Chpt. 4.3)
9	This work: Based on data from ATTO 2015, 22 November	-0.11 to -0.01	$0.04 < Da_{t_2} < 0.1$	< -0.5	$1.6 \cdot 10^{-3} \leq \nu \leq 0.2\text{Hz}$	τ_{t2} from Lagrange diffusion (see 8.); $z/z_i \approx 0.04$

Atmos. Chem. Phys. Discuss., https://doi.org/10.5194/acp-2018-1325
Manuscript under review for journal Atmos. Chem. Phys.
Discussion started: 17 May 2019

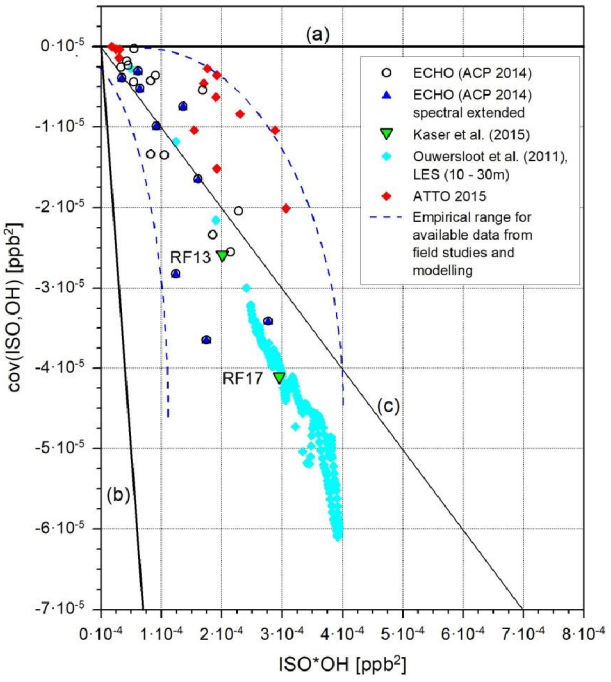

Fig. 12 The covariance between isoprene ($\boldsymbol{ISO}$) and $\boldsymbol{OH}$ as function of the product of their mean values according to Eq. (1). Line a): $\boldsymbol{I_s = 0}$; line b): $\boldsymbol{I_s = -1.0}$; line c): $\boldsymbol{I_s = -0.1}$. The data from Kaser et al. (2015) are for their measurements with PTR-MS (their Tables 1 and S2). The LES Data are from Ouwersloot et al. (2011) for the lowest layers between 10m – 30m above ground and the inhomogeneous case. The spectral extended analysis for ECHO 2003 is described in the text.

For ECHO 2003, the spectral analysis was extended to time intervals $\Delta T = 1800\ s$ to cover a range of lower frequencies of up to $5.6 \cdot 10^{-4} Hz$ (which includes larger spatial scales, if the Taylor hypothesis is applied) compared to the results for the frequency interval $1.7 \cdot 10^{-3} Hz \leq \nu \leq 0.2\ Hz$, as originally given by Dlugi et al. (2014) in their Fig. 8. By increasing the time interval, the number of values for the covariance in Fig. 12 is smaller than for the original ECHO results for $\Delta T = 600\ s$ (Dlugi et al., 2014; Fig. 8). Note that the spectral range given for $I_s(\nu)$ by Kaser et al. (2015) is for the frequency range of about $4.5 \cdot 10^{-4} Hz \leq \nu \leq 0.033\ Hz$, with an artificial extension to higher frequencies.

Extending the time interval for the ECHO 2003 case I_s becomes larger by about 18% to 27% as contributions of lower frequencies are added. As discussed by Dlugi et al. (2010), the analysis for larger time intervals than $600\ s$ was performed in the way that a symmetric linear Sawitzki-Golay low pass filter signal was subtracted from the time series (Press et al., 1991).

This method is different compared to the analysis for shorter time intervals but also fulfilled the criterion for stationarity (Beier and Weber, 1992).

In Fig. 12, almost all values of the covariance from ECHO 2003 that are smaller than $\overline{c_i' c_j'} = -2.1 \cdot 10^{-5} ppb^2$ are above the line c), which is for $I_s = -0.1$. If one numerically fits the original ECHO results (Dlugi et al. 2010, 2014), a relation, $-cov(ISO, OH) \sim \left(\overline{ISO} \times \overline{OH}\right)^n$, $n > 2$ is obtained. The contribution for frequencies below $1.7 \cdot 10^{-3} Hz$ will significantly enlarge I_s (see also Fig. 13), but does not change such a relation. The result for research flight RF13 is within this range of data from ECHO 2003. Also the results for RF17 are on the left side of line c) and even agree to results obtained by the LES modelling study of Ouwersloot et al. (2011) for the inhomogeneous distribution of emission sources. Here, results for the lowest layer between 10 m to 30 m above ground are presented. No difference is observed between modelled and observed data for this relation.

Following this non-linear relation, the segregation intensity becomes independent from the product of mean mixing ratios with increasing covariance. For example for $cov(ISO, OH) = -7 \cdot 10^{-5} ppb^2$ one estimates by this relation a mean of about $\overline{ISO} \times \overline{OH} \approx 2.5 \cdot 10^{-4} ppb^2$, and therefore, $I_s \approx -0.28$, a value in the range of the maximum estimated by Butler at al. (2008) or Kaser et al. (2015). All available data are below $\overline{ISO} \times \overline{OH} = 4 \cdot 10^{-4} ppb^2$ (Fig. 12).

The covariance is given by Eq. (2) and leads to Eq. (3). The normalized standard deviations $\sigma_i / \overline{c_i} = \sigma_{ISO} / \overline{ISO}$ and $\sigma_j / \overline{c_j} = \sigma_{OH} / \overline{OH}$ approach two bounds, a lower one for increasing mixing ratios and an upper one near the detection limits (DL) for OH and isoprene (see also Fig.6 in Dlugi at al., 2014). For example for the ECHO 2003 case and mixing ratios near DL one obtains $\sigma_{ISO}(DL)/\overline{ISO}(DL) \approx 2.6$ and $\sigma_{OH}(DL)/\overline{OH}(DL) \approx 2.8$. For increasing mixing ratios $\sigma_{ISO}/\overline{ISO} \approx 0.5$ and $\sigma_{OH}/\overline{OH} \approx 0.25$ are determined. The third term in Eq. (3) is the correlation coefficient $r_{ij} = r(ISO, OH)$, which increases with increasing product $\overline{ISO} \times \overline{OH}$ (or I_s in Fig. 9) and approaches zero for $\overline{ISO} \times \overline{OH} \to 0$ (see Fig. 7 and Fig. 8 in Dlugi et al., 2014). Therefore, even if the product of normalized standard deviations near *DL* is of the order of

$$\sigma_{ISO}(DL) \Big/ \overline{ISO}(DL) \times \sigma_{OH}(DL) \Big/ \overline{OH}(DL) \approx 2.6 \times 2.8 \approx 7.3 \,,$$

the correlation coefficient becomes small, and therefore $|I_s| < 0.07$ for such conditions. For increasing mixing ratios the correlation coefficient $r(ISO, OH)$ for ECHO 2003 is determined to be in the range (Table 3)

$$-0.5 \leq r(ISO, OH) \leq -0.6 \leq (-0.65).$$

For these conditions one obtains

$$I_s \approx r_{ISO,OH} \times \frac{\sigma_{ISO} \times \sigma_{OH}}{\overline{c_{ISO}} \times \overline{c_{OH}}} \approx -0.6 \times 0.5 \times 0.25 \approx -0.075$$

if high mixing ratios of both reactants exist together. Therefore maxima of I_s exist in between these two limits, and obviously values of $-1 \leq I_s \leq -0.35$ are not approached in an atmospheric boundary layer for conditions as found during ECHO 2003, ATTO 2015 or NOMADSS (Kaser et al., 2015). The above mentioned non-linear relation leads to an empirical upper limit of the order of $|I_s| < 0.35$ in the ABL, in agreement also with results from modelling (Table 3).

4.2.2 The Relation between Segregation Intensity and Coherent Motion

The transport and mixing processes near canopy top are controlled by non-local coherent down- and updraft eddy motion (e.g., Raupach et al., 1991, 1996; Katul et al., 1997; Cava et al., 2006). The features of coherent motion can by analyzed by the cummulant expansion method (CEM), which couples the imbalance $\Delta S_0 = S_2 - S_4$ in the contributions of *sweeps* S_2 and *ejections* S_4 to the turbulent flux, $\overline{w'\alpha'}$, of a quantity α $(= u, c_i, T)$ to the third mixed and non-mixed moments of this (vertically) transported quantity (e.g., Katul et al., 1997). Here S_2 $(w' < 0, \alpha' > 0)$ and S_4 $(w' > 0, \alpha' < 0)$ represent the quadrants II and IV of the quadrant principle (e.g., Antonia, 1981; Shaw, 1985) with the other two contributions by *outward* (S_1) and *inward* (S_3) interactions. In this way a physical turbulent transport of isoprene variance, $\overline{w'c_i'c_i'}$, is related to methods and concepts applied to the statistical analysis of time series and the probability density functions for w', α' and $\overline{w'\alpha'}$ (e.g., Nakagawa and Nezu, 1977; Raupach, 1981; Katul et al., 1997). The quantity $\overline{w'c_i'c_i'}$ is given in the divergence term $TT_{z,var}$ of Eq. (11b) and represents the influence of *ejections* S_4 as a normalized quantity $M_{21} = \left(\overline{w'c_i'c_i'}/\sigma_w\sigma_c^2\right)$ if CEM is applied.

Dlugi et al. (2014) showed that a correlation exists between the two dominant terms of the diagnostic equation for I_s (Eq. (21)), $nvar(ISO)_{is}$, and RE_{is}, and M_{21} for the ECHO 2003 case. The contribution by sweeps – represented by $M_{12} = \left(\overline{w'w'c_i'}/\sigma_w^2\sigma_c\right)$ – shows only a week correlation with $nvar(ISO)_{is}$ and RE_{is}. The same analysis on data from ATTO 2015 leads to a comparable result. In both experiments ejections (S_4), with a time duration D_e, contribute to the flux in each time interval of ten minutes. We found D_e = 34% (ECHO 2003)

and $D_e = 32\%$ (ATTO 2015) if the contributions of all quadrants are considered. For the contribution by sweeps (S_2) the time duration D_s is about 48% of the total time in each. In addition, the percentage contributions of sweeps and ejections to the total flux are comparable to their time durations and are below 100% for both experiments.

Note that the quantity $\overline{w'c_i'c_i'}$ is not given in the flux balance equation (Eq. (12)), but in the variance balance (Eq. (9)) in the divergence term TT_{var} respectively in Eq. (11a) and Eq. (11b). Even if terms $A_{h,var}$, $A_{z,var}$, II and III in Eq. (11a, 11b) were neglected, the estimation of the magnitude of the two remaining terms shows that neither the contribution of GP_{var} nor TT_{var} to the magnitude of $\overline{c_i'^2}$ is small (Table 2). Also, this analysis shows that a simple relation between I_s and one dominant term in a balance equation or by a certain process controlling the mixing of reactants does not exist. At least two or more processes can be identified, which always influence I_s in an indirect way, so that $I_s \cong -0.5$ is not reached in the field for such conditions. Therefore $|I_s|$ remains to be bounded below such values. In the following we show that such bounds of I_s are also in agreement with existing results from the field and from models, if they are presented as a function of the Damköhler number, e.g., of relations between time scales for transport/mixing and chemical reactions.

4.3 The Damköhler Dependence of the Intensity of Segregation

The relation between a transport/mixing time scale τ_t and the chemical reaction time scale, $\tau_c = \left(k_{ij} \cdot \overline{OH}\right)^{-1}$, the Damköhler number

$$Da_c = {}^{\tau_t}/_{\tau_c}$$

is commonly chosen to classify I_s (e.g., Damköhler, 1957; Astarita, 1967; Komori et al., 1991; Verver et al., 2000; Vinuesa and Vilá – Guerau de Arellano, 2005). For reaction Eq. (4) the chemical time scale τ_c is well described by the knowledge of

$$k_{ij} \approx \frac{170}{T} e^{409/T} \ [ppb^{-1}s^{-1}]$$

with a mean value of about $k_{ij} = 2.3\ ppb^{-1}s^{-1}$ in the temperature ranges for 25 July, 2003 (DOY 206) of the ECHO 2003 (Dlugi et al., 2010, 2014) and 22 November of ATTO 2015 studies. The magnitude of τ_t is often estimated by surface layer or ABL scalings (e.g., Stull, 1988; Sorbjan, 1989; Raupach, 1988). For experiments above canopies near $z = h_c$, often a time scale

Atmos. Chem. Phys. Discuss., https://doi.org/10.5194/acp-2018-1325
Manuscript under review for journal Atmos. Chem. Phys.
Discussion started: 17 May 2019

$$\tau_{t_1} \approx {}^{h_c}/_{u_*} \quad (u_* = \text{friction velocity})$$

is chosen (e.g., Patton et al., 2001). For this τ_t-scaling, Dlugi et al. (2014) determined Da_c in the range $0.01 < Da_c < 0.1$ for ECHO 2003. A revised analysis of the mixing conditions inside and directly above the mixed deciduous forest was performed based on diffusion experiments with tracer emissions at $z/h_c \approx 0.5$ and $z/h_c \approx 0.8$ during ECHO 2003. The results are compared to the wind tunnel experiments by Aubrun et al. (2005) and show that the diffusion time scale, τ_{t_2} (see also Koeltzsch, 1999), for mixing emissions from the leaves at heights $0.5 \leq z/h_c \leq 1$ to the measuring height at $z/h_c = 1.23$ is about three to four times larger than τ_{t_1}, e.g., $\tau_{t_2} \approx 3\tau_{t_1}$ (to $4\tau_{t_1}$). For illustration both time scales are given for ECHO 2003 in Fig. 13, where experimental and model results are compared (Table 3).

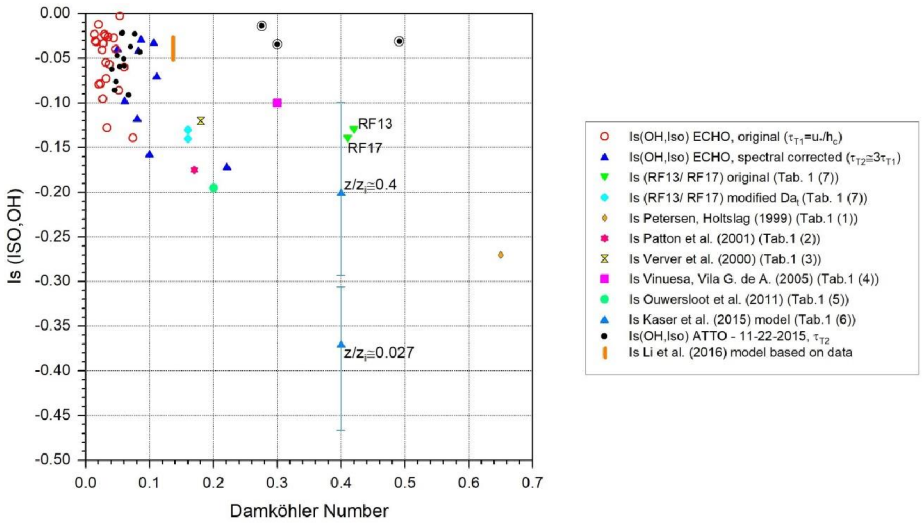

Fig. 13 The segregation intensity for reaction Eq. (4) as function of the Damköhler number $\boldsymbol{Da_c}$ for results given in Table 3 (numbers in brackets). (Three points from ATTO (circles) show smaller $\boldsymbol{I_s}$ than expected if the other data are considered. They represent low wind conditions where $\boldsymbol{u_*}$ scaling is a questionable choice and need additional analysis)

Kaser et al. (2015) give Da_c with

$$\tau_t = {}^{z_i}/_{w_*} ,$$

the ABL height z_i divided by the convective velocity scale, w_* (e.g., Stull, 1988; Garrett, 1992) for RF13 and RF17. The measurements were performed at heights near $z/z_i \approx 0.4$, and not throughout the complete ABL. Therefore, for upward-directed motion a modified estimate with $\tau_t = 0.4(z_i/w_*)$ is applied in Fig. 13 to present their data. Li et al. (2016) calculated τ_t as originally done by Kaser et al. (2015). They present I_s- maxima for

Atmos. Chem. Phys. Discuss., https://doi.org/10.5194/acp-2018-1325
Manuscript under review for journal Atmos. Chem. Phys.
Discussion started: 17 May 2019

$z/z_i \approx 300\,m/2100\,m \approx 0.14$. Therefore, with $\tau_t \approx 0.14(z_i/w_*)$ their results agree to the range of other data in Fig. 13.

The model data (Table 3; Fig. 13) of Kaser et al. (2015) are given with their complete range for $z/z_i \approx 0.4$ and the canopy top values for $z/z_i \approx 0.027$. Their near-surface values of I_s are significantly larger than any other data for canopy top flow or surface layer conditions in the literature (e.g., Ouwersloot et al., 2011; Vinuesa and Vilà-Guerau de Arellano, 2005; Patton et al., 2001, Kim et al., 2016). Without the model data for $z/z_i \approx 0.027$, all other results agree with a non-linear increase of I_s with increasing Da_c and the existence of a limiting range of about $I_s < -0.35$ for $0.5 \leq Da_c \leq 2$ (Fig. 13). This empirical result agrees also with the numerical fit according to a power function as shown in Fig. 12.

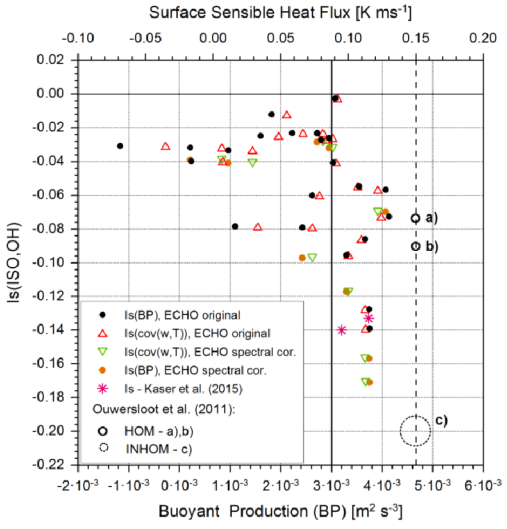

Fig. 14 The intensity of segregation as a function of buoyant production ($\boldsymbol{BP}$) and the sensible heat flux $\boldsymbol{H}$. The dotted circle (c)) and the data points labeled a) and b) indicate the range of results presented by Ouwersloot et al. (2011) for homogeneous (HOM) and inhomogeneous (INHOM) source distribution on the land surface. Also the average values reported by Kaser et al. (2015) agree with this approach if the results from our CBL scaling analysis for $\boldsymbol{H}$ are applied. $\boldsymbol{H > 0.078\,K\,m\,s^{-1}}$ and $\boldsymbol{BP > 3 \cdot 10^{-3} m^2\,s^{-1}}$ describe the onset of convective conditions at canopy top.

In addition, $I_s(ISO, OH)$ can be empirically related to the buoyant production, BP, and also to the turbulent sensible heat flux, H_s, near the surface (Dlugi et al., 2014). The agreement with model results povided by Ouwersloot et al. (2011) becomes better (Fig. 14), if lower frequency contributions are added as mentioned above (Fig. 12, 13). This spectral correction with respect to the original ECHO results covers also the spectral range of I_s given by Kaser

et al. (2015), if the results from our CBL-scaling analysis for the sensible heat flux are applied to their average I_s values (Fig. 14). Note that the data from ECHO 2003 in the range of $BP > 3 \cdot 10^{-3} m^2\, s^{-3}$ represent NO_x mixing ratios below $2\, ppb$. The NOMADSS flights were performed in air masses with mean NO_x mixing ratios below about $0.6\, ppb$.

5. Summary and Conclusion

The published results from field studies on segregation and the new measurements from the ATTO site for the reaction of isoprene with OH are discussed and compared to models. Some statements made by Kaser et al. (2015) for their study in the ABL are compared to the available relationships obtained from the data analysis of field studies near canopy top and in the ABL to give a comprehensive overview and to identify possible natural limits on I_s based on theoretical considerations and the data available so far.

The intensity of segregation, I_s, appears to be (weakly) proportional to the isoprene flux only near canopy top, in agreement with an analysis for other scalar quantities described in the literature (see: Sections 3.3 and 4.1). For larger heights above the surface, this correlation becomes small, as not only the production term GP_{var} but also other terms contribute to the budget of isoprene variance as discussed in Section 3.3 and Section 4.1. An increase of I_s with increasing standard deviation of isoprene $\sigma_i = \overline{(c_i'^2)}^{1/2}$ is observed near canopy top and also reported from modelling (e.g., Patton et al., 2001; Ouwersloot et al., 2011), but this increase is not exclusively related to an increasing isoprene flux.

In addition, the covariance $\overline{c_i' c_j'} = \overline{ISO' OH'}$ is non-linearly related to the product of the mean mixing ratios, $\overline{c_i} \times \overline{c_j} = \overline{ISO} \times \overline{OH}$. The data show an empirical relation of a power-law type (Fig. 12). This relation points towards an upper bound for I_s of about $|I_s| < 0.35$ near canopy top as well as in the ABL, a value which is most likely also related to the behavior of the correlation coefficient r_{ij} with increasing mixing ratios and I_s (Fig. 9). Therefore, the relation between experimentally determined $r_{ij,exp}$ and correlation coefficients applied or determined in model studies, $r_{ij,mod}$, $|r_{ij,exp}| < |r_{ij,mod}|$ needs further analysis. A comparable empirical upper limit for $I_s = f(Da_c)$ is obtained if experimental and model results of I_s are analyzed as function of the Damköhler number, Da_c. The empirical upper limit $|I_s| < 0.35$ is approached for $0.5 \leq Da_c \leq 2$. An extended analysis of the ECHO 2003 data proves that I_s has significant

contributions in the frequency range between $4.5 \cdot 10^{-4} Hz$ to $1.0 \cdot 10^{-3} Hz$. Therefore absolute values of I_s increase by at least 15% compared to the results described by Dlugi et al (2014) for the range $1.7 \cdot 10^{-3} Hz \leq r \leq 0.2\ Hz$. This trend is qualitatively visible in Fig. 13, with a tendency for surface measurements with smaller $|I_s|$ than given by modelling results that integrate over the ABL. Aircraft measurements that are also influenced by landscape heterogenity exhibit relatively large values for I_s.

For the calculation of Da_c the concepts applied to determine the transport/mixing time scale need further analysis, as a simple formula like $\tau_{t_1} = h_c/u_*$ (or $\tau_{t_1} = z_i/w_*$) underestimates the time scales obtained from an analysis of diffusion experiments, at least for ECHO 2003 and qualitatively also for the ATTO site.

It can be shown that for both case studies, ECHO 2003 and ATTO 2015, the contribution of ejections to the turbulent isoprene flux correlates with the two dominant terms $nvar(ISO)_{is}$ and RE_{is} in the diagnostic equation for I_s. If in general only ejections contribute to I_s for a compound emitted by an inhomogeneous source, the magnitude of $|I_s|$ will be proportional to the percentage amount of ejections.

The observed increase of I_s with increasing buoyant production, BP, respectively with increasing surface sensible heat flux (Fig. 14) (Dlugi et al., 2014), is further improved if the extended spectral analysis for ECHO 2003 is compared to results from Kaser et al. (2015) and model data from Ouwersloot et al. (2011). Here, the surface sensible heat fluxes, H_s, were calculated from Fig. S6 in Kaser et al. (2015) by CBL scaling for fluxes, as discussed in Section 3. Both results for the isoprene flux as well as the sensible heat flux are also comparable to measured fluxes in the same region as described by Su et al. (2015). Although there is no simple direct relation between I_s and BP - as given by a balance equation - higher values of I_s seem to appear generally at higher BP and H_s for convective conditions.

In summary, there are still only few measurements of segregation intensity (two ground based and one aircraft campaign), but in line with modelling studies some general tendencies could be established. Surface measurements show mostly I_s less than 18 % for 10-min values. In line with the modelling studies and the aircraft measurements, by including longer time scales (lower freqencies) or larger spatial scales, I_s reaches larger values between 10 and 20 % (some extremes up to 30 %), also in line with a spectral representation of I_s given by Kaser et al. (2015). Therefore, one could argue that I_s is scale dependent for comparable turbulent conditions with, as a hypothesis,

$$\left|I_{s\_homogeneous\ surface}\right| \leq \left|I_{s\_inhomogeneous\ surface}\right| .$$

Some of the above findings may be particular to the considered reaction, as OH mixing ratios are always low compared to isoprene and both compounds exhibit a similar diurnal cycle driven by radiation (OH) and surface temperature (isoprene) which also serves to generate convection and turbulence, This might be one reason for the limits for I_s observed for this reaction in the boundary layer.

Author contribution:

RD, MB, MZ, HH, MA and MS initiated the study and developed the scientific concept of the study. RD, MB, CM, AT, MZ, OA, EB, AH, JK, GK, DM, MM, AN,EP, FR, ST, JW, AY-S, HH and MS performed the measurements and/or contributed to the data analysis with major contributions to study design, measurement setup, measurements and data analysis from ATTO and ECHO. HO contributed modeling results. All authors contributed to the discussion and interpretation of the results and to the writing of the paper.

Competing interests:
The authors declare that they have no conflict of interest.

Data availability: Data used in this publication can be accessed by contacting the corresponding authors. General information on the ATTO project as well as a link to the ATTO-data portal can be found at https://www.attoproject.org/.

Acknowledgement:

We thank the Max Planck Society and the Instituto Nacional de Pesquisas da Amazonia for continuous support. We acknowledge the support by the German Federal Ministry of Education and Research (BMBF contract 01LB1001A) and the Brazilian Ministéro de Ciência Technologia e inovação (MCTI/FINEP contract 01.11.01248.00) as well as the Amazon State University (UEA), FAPEAN, LBA/INPA and SDS/CEUC/RDS-Uatumã.

Ralph Dlugi, Martina Berger and Michael Zelger greatly acknowledge the financial support by the Max Planck Institute for Chemistry.

Nelson Luís Dias contributed by a very valuable discussion on concepts and methods of data analysis. We thank Thomas Klüpfel, Markus Rudolf, Michael Welling, Dieter Scharffe, Reiner Ditz, Stefan Wolff, Stephan Keßel, Thómas Chor and Lucas Emilio B. Hoeltgebaum for various supports preparing and performing the field study at the ATTO site, for data pre-processing and pre- analysis and Nicole Mölders and Eiko Nemitz for intensive discussion on various aspects of these topics.

References

André, J. C., De Moor, G., Lacarrère, P., and du Vachat, R.: Modeling the 24-Hour Evolution of the Mean and Turbulent Structures of the Planetary Boundary Layer, J. Atmos. Sci., 35, 1861 – 1883, https://doi.org/10.1175/1520-0469(1978)035<1861:MTHEOT>2.0.CO;2, 1978

Andreae, M. O. Acevedo, O. C., Araùjo, A., Artaxo, P.,Barbosa, C. G. G.,Barbosa, H. M. J., Brito, J., Carbone, S.,Chi, X., Cintra, B. B. L., da Silva, N. F.,Dias, N. L., Dias-Júnior, C. Q.,Ditas, F., Ditz, R.,Godoi, A. F. L., Godoi, R. H. M., Heimann, M., Hoffmann, T., Kesselmeier, J., Könemann, T., Krüger, M. L., Lavric, J. V., Manzi, A. O., Moran-Zuloaga, D., Nölscher, A. C., Santos Nogueira, D., Piedade, M. T. F., Pöhlker, C., Pöschl, U., Rizzo, L. V., Ro, C.-U., Ruckteschler, N., Sá, L. D. A., Sá, M. D. O., Sales, C. B., Santos, R. M. N. D., Saturno, J., Schöngart, J., Sörgel, M., de Souza, C. M., de Souza, R. A. F.,Su, H., Targhetta, N., Tóta, J., Trebs, I., Trumbore, S., van Eijck, A., Walter, D., Wang, Z., Weber, B., Williams, J., Winderlich, J., Wittmann, F., Wolff, S., and Yáñez-Serrano, A. M.: The Amazon Tall Tower Observatory (ATTO) in the remote Amazon Basin: overview of first results from ecosystem ecology, meteorology, trace gas, and aerosol measurements, Atmos. Chem. Phys. Discuss., 15, 11599–11726, https://doi:10.5194/acpd-15-11599-2015, 2015

Antonia, R.A.: Conditional sampling in turbulence measurement. Ann. Rev. Fluid Mech. 13:131-156, https://doi.org/10.1146/annurev.fl.13.010181.001023, 1981

Ammann, C., Spirig, C., Neftel, A., Steinbacher, M., Komenda, M., and Schaub, A.: Application of PTR-MS for measurements of biogenic VOC in a deciduous forest, Int. J. Mass Spectrom., 239, 87–101, 2004

Astarita, G.: Mass transfer with chemical reaction, Elsevier, Amsterdam, 1967

Aubrun, S., Koppmann, R., Leitl, B., Möllmann-Coers, M., and Schaub, A.: Physical modelling of a complex forest area in a wind tunnel – comparison with field data, Agr. Forest. Meteorol., 129, 121–135, 2005

Beier, N., and Weber, M.: Turbulente Austauschprozesse in der Grenzschicht. Technical Report, Meteorologisches Institut, Universität München, Germany, 1992

Bencula, K., and Seinfeld, J.: On frequency distributions of air pollutant concentrations, Atmos. Environ., 10, 941–950, 1976

Brune, W. H., Stevens, P. S., and Mather, J. H.: Measuring OH and HO_2 in the Troposphere by Laser-Induced Fluorescence at Low-Pressure, J Atmos Sci, 52, 3328-3336, https://doi 10.1175/1520-0469(1995)052<3328:Moahit>2.0.Co;2, 1995

Businger, J. A.: Turbulent transfer in the atmospheric surface layer. In: D. A. Hangen (Ed.): Workshop on Micrometeorology, Chapter 2, AMS, Bosten, USA, 1973

Butler, T. M., Taraborrelli, D., Brühl, C., Fischer, H., Harder, H., Martinez, M., Williams, J., Lawrence, M. G., and Lelieveld, J.: Improved simulation of isoprene oxidation chemistry with the ECHAM5/MESSy chemistry-climate model: lessons from the GABRIEL airborne field campaign, Atmos. Chem. Phys., 8, 4529–4546, https://doi:10.5194/acp-8-4529-2008, 2008

Caughey, S. J., and Palmer, S. G.: Some aspects of turbulence structure through the depth of the convective boundary layer, Quart J. Roy. Meteor. Soc., 105, 811-827, https://doi:10.1002/qj.49710544606, 1979

Cava, D., Katul, G. G., Scrimieri, A., Poggi, D., Cescatti, A., and Giostra, U.: Buoyancy and the sensible heat flux budget within dense canopies, Boundary Layer Meteorol., 118, 217 – 240, https://doi: 10.1007/s10546-005-4736-1, 2006

Ciccioli, P., Fabozzi, C., Brancaleoni, E., Cecinato, A., Frattoni, M., Loreto, F., Kesselmeier, J., Schäfer, L., Bode, K., Torres, L., and Fugit, J.-L.: Use of the isoprene algorithm for predicting the monoterpene emission from the Mediterranean holm oak Quercus ilex L.: Performance and limits of this approach, J. Geophys. Res., 102, 23319–23328, 1997

Crosley, D. R.: The Measurement of Oh and Ho2 in the Atmosphere, J Atmos Sci, 52, 3299-3314, https://doi 10.1175/1520-0469(1995)052<3299:Tmooah>2.0.Co;2, 1995

Cuijpers, J. W. M. and Holtslag, A. A. M.: Impact of Skewness and Nonlocal Effects on Scalar and Buoyancy Fluxes in Convective Boundary Layers. J. Atmos. Sci., 55: 151-162, 1998

Damköhler, G.: Einfluß von Diffussion, Strömung und Wärmetransport auf die Ausbeute bei chemisch-technischen Reaktionen, VDI, Leverkusen, Germany, 126 pp., 1957

Danckwerts, P.: The definition and measurement of some characteristics of mixtures, Appl. Sci. Res., 3, 279–296, 1952

Deardorff, J. W.: Three-dimensional numerical study of turbulence in an entraining mixed layer, Boundary Layer Meteorol., 7, 199 – 223, https://doi.org/10.1007/BF00227913, 1974

Dlugi, R., Berger, M., Zelger, M., Hofzumahaus, A., Siese, M., Holland, F., Wisthaler, A., Grabmer, W., Hansel, A., Koppmann, R., Kramm, G., Möllmann-Coers, M., and Knaps, A.: Turbulent exchange and segregation of HOx radicals and volatile organic compounds above a deciduous forest, Atmos. Chem. Phys., 10, 6215–6235, https://doi:10.5194/acp-10-6215-2010, 2010

Dlugi, R. , Berger, M., Zelger, M., Hofzumahaus, A., Rohrer, F., Holland, F., Lu, K., and Kramm, G.: The balances of mixing ratios and segregation intensity: a case study from the field (ECHO 2003), Atmos. Chem. Phys., 14, https://doi:10.5194/acp-14-10333-2014, 2014

Donaldson, C. D.: On the modelling of the scalar correlation necessary to construct a second order closure description of turbulent reacting flows, in: A review in turbulent mixing in non reactive and reactive flows, edited by: Murthy, S., Plenum Press, New York, 1975

Donaldson, C. D., and Hilst, G.: Effect of inhomogeneous mixing on atmospheric photochemical reactions, Environ. Sci. Technol., 6, 812–816, 1972

Doughty, C. E., and M. L. Goulden: Are tropical forests near a high temperature threshold?, J. Geophys. Res., 113, G00B07, https://doi:10.1029/2007JG000632, 2008

Ebel, A., Memmesheimer, M., and Jakobs, H. J.: Chemical perturbations in the planetary boundary layer and their relevance for chemistry transport modelling, Bound.-Lay. Meteorol., 125, 256–278, 2007

Eerdekens, G., Ganzeveld, L., Vilà-Guerau de Arellano, J., Klüpfel, T., Sinha, V., Yassaa, N., Williams, J., Harder, H., Kubistin, D., Martinez, M., and Lelieveld, J.: Flux estimates of isoprene, methanol and acetone from airborne PTR-MS measurements over the tropical rainforest during the GABRIEL 2005 campaign, Atmos. Chem. Phys., 9, 4207-4227, https://doi.org/10.5194/acp-9-4207-2009, 2009

Finlayson-Pitts, B. J. and Pitts Jr., J. N.: Atmospheric Chemistry: Fundamentals and Experimental Techniques, J. Wiley & Sons, New York, 1986

Garratt, J. R.: The Atmospheric Boundary Layer, Cambridge University Press, UK, 1992

Gerken, T., Chamecki, M., and Fuentes, J. D.: Estudo da interação entre o transporte de compostos orgânicos voláteis biogênicos e química dentro de um dossel da floresta tropical utilizando

Large Eddy Simulation, Ciência e Natura, Santa Maria v.38 Ed. Especial- IX Workshop Brasileiro de Micrometeorologia, p. 262 – 265, https://doi: 10.5902/2179460X21577, 2016

Guenther, A. , Hewitt, C. N., Erickson, D., Fall, R., Geron, C., Graedel, T., Harley, P., Klinger, L., Lerdau, M., Mckay, W. A., Pierce, T., Scholes, B., Steinbrecher, R., Tallamraju, R., Taylor, J., and Zimmerman, P. : A global model of natural volatile organic compound emissions, J. Geophys. Res., 100, 8873–8892, https://doi.org/10.1029/94JD02950, 1995

Guenther, A. B., Jiang, X., Heald, C. L., Sakulyanontvittaya, T., Duhl, T., Emmons, L. K., and Wang, X. : The Model of Emissions of Gases and Aerosols from Nature version 2.1 (MEGAN2.1): an extended and updated framework for modeling biogenic emissions: Geoscientific Model Development, 5, 1471-1492, https://doi:10.5194/gmd-5-1471-2012, 2012

Hard, T. M., Obrien, R. J., Chan, C. Y., and Mehrabzadeh, A. A.: Tropospheric Free-Radical Determination by Fage, Environ Sci Technol, 18, 768-777, https://doi:10.1021/es00128a009, 1984

Haugen, D. A., (Ed.): Workshop on Micrometeorology, Amer. Meteor. Soc., 45 Beacon St., Boston, MA 02108. 392pp., 1973

Hens, K., Novelli, A., Martinez, M., Auld, J., Axinte, R., Bohn, B., Fischer, H., Keronen, P., Kubistin, D., Nölscher, A. C., Oswald, R., Paasonen, P., Petaja, T., Regelin, E., Sander, R., Sinha, V., Sipila, M., Taraborrelli, D., Ernest, C. T., Williams, J., Lelieveld, J., and Harder, H.: Observation and modelling of HOx radicals in a boreal forest, Atmospheric Chemistry and Physics, 14, 8723-8747, https://doi:10.5194/acp-14-8723-2014, 2014

Hess, G.D.: Observations and scaling of the atmospheric boundary layer, Aust. Met. Mag., 41: 79-99, 1992

Heus, T., and Jonker, H. J. J.: Subsiding Shells around Shallow Cumulus Clouds, J. of the Atmos. Sci., 65, 1003 – 1017, https://doi:10.1175/2007JAS2322.1, 2008

Higgins, C. W., Katul, G. G., Froidevaux, M., Simeonov, V., and Parlange, M.B.: Are atmospheric surface layer flows ergodic? Journal, Geophysical Research Letters, 40, 3342–3346, https://doi: 10.1002/grl.50642, 2013

Hornbrook, R. S. , Crawford, J. H., Edwards, G. D., Goyea, O., Mauldin III, R. L., Olson, J. S., and Cantrell, C. A.: Measurements of tropospheric HO_2 and RO_2 by oxygen dilution modulation and chemical ionization mass spectrometry, Atmos. Meas. Tech., 4, 735-756, https://doi.org/10.5194/amt-4-735-2011, 2011

Jiménez-Muñoz, J. C., Mattar, C., Barichivich, J., Santamaría-Artigas, A., Takahashi, K., Malhi, Y., Sobrino, J. A., and van der Schrier, G.: Record-breaking warming and extreme drought in the Amazon rainforest during the course of El Niño 2015-2016, Scientific reports 6, 33130, https://doi:10.1038/srep33130, 2016

Kaimal, J. C., and Finnigan, J. J.: Atmospheric Boundary Layer Flows: Their Structure and Measurement, Oxford University Press, New York/Oxford, 289 pp., 1994

Karl, T. G. , Guenther, A., Yokelson, R. J., Greenberg, J., Potosnak, M., Blake, D. R., and Artaxo, P.: The tropical forest and fire emissions experiment: Emission, chemistry, and transport of biogenic volatile organic compounds in the lower atmosphere over Amazonia, J. Geophys. Res., 112, D18302, https://doi.org/10.1029/2007JD008539, 2007

Karl, T., Misztal, P. K., Jonsson, H. H., Shertz, S., Goldstein, A. H., and Guenther, A. B.: Airborne flux measurements of BVOCs above Californian oak forests: Experimental investigation of surface and entrainment fluxes, OH densities, and Damköhler numbers, J. Atmos. Sci., 70, 3277–3287, https://doi:10.1175/JAS-D-13-054.1, 2013

Kaser, L. , Karl, T., Yuan, B., Mauldin III, R. L., Cantrell, C. A., Guenther, A. B., Patton, E. G., Weinheimer, A. J., Knote, C., Orlando, J., Emmons, L., Apel, E., Hornbrook, R., Shertz, S.,

Ullmann, K., Hall, S., Graus, M., de Gouw, J., Zhou, X., and Ye, C.: Chemistry-turbulence interactions and mesoscale variability influence the cleansing efficiency of the atmosphere, Geophys. Res. Lett., 42 : 10,894 – 10,903, https://doi: 10.1002/2015GL066641, 2015

Katul, G.G, Hsieh, Ch. I., Kuhn, G., Ellsworth, D., and Nie, D.: Turbulent eddy motion at the forest-atmosphere interface. J Geophys Res 102: 13409-13421, 1997

Kesselmeier, J.: Exchange of Short-Chain Oxygenated Volatile Organic Compounds (VOCs) between Plants and the Atmosphere: A Compilation of Field and Laboratory Studies, J. Atmos. Chem., 39(3), 219 – 233, 2001

Kesselmeier, J., and Staudt, M.: Biogenic volatile organic compounds (VOC): An overview on emission, physiology and ecology, J. Atmos. Chem., 33, 23–88,1999

Kim, S.-W., Barth, M. C., and Trainer, M.: Impact of turbulent mixing on isoprene chemistry, Geophys. Research Letters, 43, 7701 – 7708, https://doi:10.1002/2016GL069752, 2016

Koeltzsch, K.: On the relationship between the Lagrangian and Eulerian time scale, Atmos. Environment, 33: 117-128, 1998

Komori, S., Kanzaki, T., and Morakami, Y.: Simultaneous measurements on instantaneous concentrations of two reacting species in a turbulent flow with a rapid reaction, Phys. Fluids, A3, 507–510, 1991

Krol, M. C., Molemaker, M.-J., and Vilà Guerau de Arellano, J.: Effects of turbulence and heterogeneous emission on photochemically active species in the convective boundary layer, J. Geophys. Res., 105, 6871–6884, https://doi:10.1029/1999JD900958, 2000

Kramm, G.: Zum Austausch von Ozon und reaktiven Stickstoffverbindungen zwischen Atmosphäre und Biosphäre, Thesis, Humboldt Universty, Berlin, published as: Schriftenreihe des Fraunhofer-Instituts für Atmosphärische Umweltforschung, 34, ISBN: 3-927548-75-8, 1995

Kramm, G., and Meixner, F. X.: On the dispersion of trace species in the atmospheric boundary layer: A re-formulation of the governing equations for the turbulent flow of the compressible atmosphere, Tellus, 52A, 500–522, 2000

Lamb, R., and Seinfeld, J.: Modeling for urban air pollution – general theory, Environ. Sci. Technol., 7, 253–261, 1973

Lamb, R., and Shu, W.: A Model of second order chemical reactions in turbulent fluid – part I: Formulation and Validation, Atmos. Environ., 12, 1685–1694, 1978

Lang, A. R. G., and Bradley, E. F.: Pressure covariance terms in the heat and moisture flux equations for local advection, Proc. 8th Australasien Fluid Mechanics Conference, Univ. of Newcastel, N.S.W., 28 November/ 2 December 1983, p. 1A.1 – 1A.4, 1983

Launder, B.E.: Heat and mass transport in Turbulence (ed. P. Bradshaw), 2nd edn., Springer Verlag, New York, 1978

Lenschow, D. H. , Wyngaard, J. C., and Pennell, W. T.: Mean-Field and Second-Moment Budgets in a Baroclinic, Convective Boundary Layer, J. Atmos. Sci., 37, 1313–1326, https://doi.org/10.1175/1520-0469(1980)037<1313:MFASMB>2.0.CO;2, 1980

Lenschow, D. H.: Reactive trace species in the boundary layer from a micrometeorological perspective, J. Meteorol. Soc. Jpn., 60, 472–480, 1982

Li, Y. , Barth, M. C., Chen, G., Patton, E. G., Kim, S.-W., Wisthaler, A., Mikoviny, T., Fried, A., Clark, R., Steiner, A. L.: Large-eddy simulation of biogenic VOC chemistry during the DISCOVER-AQ 2011 campaign, J. of Geophys. Research: Atmosphere, 121(13), 8083–8105, https://doi:10.1002/2016JD024942, 2016

Mallik, C., Tomsche, L., Bourtsoukidis, E., Crowley, J. N., Derstroff, B., Fischer, H., Hafermann, S., Hueser, I., Javed, U., Kessel, S., Lelieveld, J., Martinez, M., Meusel, H., Novelli, A., Phillips, G. J., Pozzer, A., Reiffs, A., Sander, R., Taraborrelli, D., Sauvage, C., Schuladen, J., Su, H., Williams, J., and Harder, H.: Oxidation processes in the Eastern Mediterranean atmosphere: Evidence from the Modelling of HOx Measurements over Cyprus, Atmos. Chem. Phys., 2018, 1-35, https://doi:10.5194/acp-2018-25, 2018.

Mao, J., Ren, X., Zhang, L., Van Duin, D. M., Cohen, R. C., Park, J. H., Goldstein, A. H., Paulot, F., Beaver, M. R., Crounse, J. D., Wennberg, P. O., DiGangi, J. P., Henry, S. B., Keutsch, F. N., Park, C., Schade, G. W., Wolfe, G. M., Thornton, J. A., and Brune, W. H.: Insights into hydroxyl measurements and atmospheric oxidation in a California forest, Atmospheric Chemistry and Physics, 12, 8009-8020, https://doi:10.5194/acp-12-8009-2012, 2012

Martinez, M., Harder, H., Kubistin, D., Rudolf, M., Bozem, H., Eerdekens, G., Fischer, H., Klupfel, T., Gurk, C., Konigstedt, R., Parchatka, U., Schiller, C. L., Stickler, A., Williams, J., and Lelieveld, J.: Hydroxyl radicals in the tropical troposphere over the Suriname rainforest: airborne measurements, Atmospheric Chemistry and Physics, 10, 3759-3773, 2010

Mauldin III, R.L., Cantrell, C. A., Zondlo, M., Kosciuch, E., Eisele, F. L., Chen, G., Davis, D., Weber, R., Crawford, J., Blake, D., Bandy, A., and Thornton, D.: Highlights of OH, H_2SO_4, and methane sulfonic acid meas-urements made aboard the NASA P-3B during Transport and Chemical Evolution over the Pacific, J. Geophys. Res., 108(D20), 8796, https://doi.org/10.1029/2003JD003410, 2003

McBean, G. A., and Miyake, M.: Turbulent transfer mechanisms in the atmospheric surface layer, Quart. J. Meteorol, Soc., 98, 383 – 398, https://doi:10.1002/qj.49709841610, 1972

McRae, G., Goodin, W., and Seinfeld, J.: Mathematical modelling of photochemical air pollution, EQL-Report No.18, Tech. rep., California Inst.of Technology, Pasadena, 1982

Moeng, C.-H., and Sullivan, P. P.: A comparison of shear- and buoyancy-driven planetary boundary layer ows. J. Atmos. Sci., **51,** 999–1022, 1994

Moeng, C.-H., and Wyngaard, J. C.: Statistics of conservative scalars in the convective boundary layer. J. Atmos. Sci., 41:3161 – 3169, 1984

Molemaker, M. J., and Vilà-Guerau de Arellano, J.: Control of chemical reactions by convective turbulence in the boundary layer. J. Atmos. Sci., 55, 568-579, 1998

Monin, A. S., and Obukhov, A. M.: Basic laws of turbulent mixing in the surface layer of the atmosphere. Trans. Geophys. Inst. Akad. Nauk. USSR, 151, 163–187, 1954

Monin, A. S., and Yaglom, A. M.: Statistical fluid mechanics, M.I.T. Press, Cambridge, Mass, 1971

Müller, J.-F., Stavrakou, T., Wallens, S., De Smedt, I., Van Roozendael, M., Potosnak, M. J., Rinne, J., Munger, B., Goldstein, A., and Guenther, A. B.: Global isoprene emissions estimated using MEGAN, ECMWF analyses and a detailed canopy environment model, Atmos. Chem. Phys., 8, 1329–1341, https://doi.org/10.5194/acp-8-1329-2008, 2008

Nakagawa, H., and Nezu, I.: Prediction of the contributions to the Reynolds stress from bursting events in open-channel flows, J. Fluid Mech. 80, 99-128, https://doi.org/10.1017/S0022112077001554, 1977

Nölscher, A.C., Yañez-Serrano, A.M., Wolff, S., Carioca de Araujo, A., Lavriĉ, J.V., Kesselmeier, J., and Williams, J.: Unexpected seasonality in quantity and composition of Amazon rainforest air reactivity, nature communication, 7:10383, https://doi:10.1038/ncomms10383, 2015

Novelli, A., Hens, K., Ernest, C. T., Kubistin, D., Regelin, E., Elste, T., Plass-Dulmer, C., Martinez, M., Lelieveld, J., and Harder, H.: Characterisation of an inlet pre-injector laser-induced fluorescence instrument for the measurement of atmospheric hydroxyl radicals, Atmos Meas Tech, 7, 3413-3430, https://doi.org/10.5194/amt-7-3413-2014, 2014

O'Brien, E. E.: Turbulent mixing of two rapidly reacting chemical species, Phys. Fluids, 14, 1326–1331, 1971

Ouwersloot, H. G. , Vilà-Guerau de Arellano, J., van Heerwaarden, C. C., Ganzeveld, L. N., Krol, M. C., and Lelieveld, J.: On the segregation of chemical species in a clear boundary layer over heterogeneous land surfaces, Atmos. Chem. Phys., 11, 10681 – 10704, https://doi.org/10.5194/acp-11-10681-2011, 2011

Ouwersloot, H. G., Vilà–Guerau de Arellano, J., van Stratum, B. J. H., Krol, M. C., and Lelieveld, J.: Quantifying the transport of subcloud layer reactants by shallow cumulus clouds over the Amazon, J. Geophys. Res., 118, 13.041–13.059, https://doi.org/10.1002/2013JD020431, 2013

Patton, E. G., Davis, K.J., Barth, M.C., and Sullivan, P.P: Decaying scalars emitted by a forest canopy: A numerical study, Bound-Lay. Meteorol., 100, 91–129, 2011

Patton, E. G., Sullivan, P. P., and Davis, K. J.: The influence of a forest canopy on top-down and bottom-up diffusion in the planetary boundary layer. Q. J. R. Meteorol. Soc., 129: 1415 – 1434, https://doi.org/10.1256/qj.01.175, 2003

Panofsky, H. A. and Dutton, J. A.: Atmospheric Turbulence. J. Wiley, New York, 397 p., 1984

Poggi, D., Katul, G. G., and Albertson, J. D.: Momentum transfer and turbulent kinetic energy budgets within a dense model canopy, Boundary-Layer Meteorology, 111(3), 589-614 https://doi.org/10.1023/B:BOUN.0000016502.52590.af, 2004

Pugh, T. A. M., MacKenzie, A. R., Langford, B., Nemitz, E., Misztal, P. K., and Hewitt, C. N.: The influence of small-scale variations in isoprene concentrations on atmospheric chemistry over a tropical rainforest, Atmos. Chem. Phys., 11, 4121–4134, https://doi.org/10.5194/acp-11-4121-2011, 2011

Ramos da Silva, R., Gandu, A. W., Sa´, L. D. A., and Dias, M. A. F.: Cloud streets and land–water interactions in the Amazon, Biogeochemistry, 105, 201–211, https://doi.org/10.1007/s10533-011-9580-4, 2011

Raupach, M. R.: Conditional statistics of Reynolds stress in rough-wall and smooth-wall turbulent boundary layers, J. Fluid Mech., 108, 363 – 382, https://doi.org/10.1017/S0022112081002164, 1981

Raupach, M. R.: Canopy transport processes, in: Flow and Transport in the Natural Environment: Advances and Applications, edited by: Steffen, W. L. and Denmead, O. T., Springer, Berlin, Germany, 95–127, 1988

Raupach, M. R., Antonia, R. A., and Rajagopalan, S.: Rough-wall turbulent boundary layers. Appl. Mech. Rev., 44:1 – 25, 1991

Raupach, M. R., Finnigan, J. J., and Brunet, Y.: Coherent eddies and turbulence in vegetation canopies: The mixing layer analogy, Bound.-Lay. Meteorol., 78, 351–382, 1996

Reynolds, O.: On the Dynamical Theory of Incompressible Viscous Fluids and the Determination of the Criterion, Phil. Trans. Roy. Soc. London, A 186, 123 – 164, (Roy. Soc., https://doi.org/10.1098/rsta.1895.0004), 1895

Richardson, L. F.: The Supply of Energy from and to Atmospheric Eddies, Proc. Roy. Soc., A, 97, 354 – 373 (Roy. Soc., https://doi.org/10.1098/rspa.1920.0039), 1920

Rohrer, F., Lu, K., Hofzumahaus, A., Bohn, B., Brauers, T., Chang, C.-C., Fuchs, H., Häseler, R., Holland, F., Hu, M.,Kita, K., Kondo, Y., Li, L., Lou, S., Oebel, A., Shao, M., Zeng, L., Zhu, T., Zhang, Y., and Wahner, A.: Maximum efficiency in the hydroxyl-radical-based self-cleansing of the troposphere, Nature Geoscience, 7, 559–563, https://doi:10.1038/ngeo2199, 2014

Sachs, L., and Hedderich, J.: Angewandte Statistik, Springer, Berlin, Heidelberg, New York, 2006

Schaub, A.: Untersuchung von Isopren und dessen Oxidationsprodukten in und oberhalb eines Mischwaldes, Ph.D. thesis, Mathematisch-Naturwissenschaftliche Fakultät, Universität Köln, Germany, 2007

Schumann, U.: Large-eddy simulation of turbulent diffusion with chemical reactions in the convective boundary layer, Atmos. Environ., 23, 1713–1729, 1989

Seinfeld, J. H. and Pandis, S. N.: Atmospheric Chemistry and Physics, John Wiley & Sons, New York/Chichester/Weilheim/Brisbane/Singapore/Toronto, 1997

Shaw, R.H. , Paw, K. T. U., Zhang, X. J., Gao, W., Den Hartog, G., Neumann, H. H.: Retrieval of turbulent pressure fluctuations at the ground surface beneath a forest, Boundary Layer Meteorol., 50, 319 – 338, https://doi.org/10.1007/BF00120528, 1990

Shu, W.: Turbulent chemical reactions: Application to atmospheric chemistry, Ph.D. thesis, Dept. Chem. Eng., Caltec, Pasadena, 1976

Sindelarova, K., Granier, C., Bouarar, I., Guenther, A., Tilmes, S., Stavrakou, T., Muller, J. F., Kuhn, U., Stefani, P., and Knorr, W.: Global data set of biogenic VOC emissions calculated by the MEGAN model over the last 30 years, Atmos. Chem. Phys., 14, 9317-9341, https://doi.org/10.5194/acp-14-9317-2014, 2014

Sorbjan, Z.: Structure of the atmospheric boundary layer, Prentice Hall, N. J., USA, 1989

Spirig, C., Neftel, A., Ammann, C., Dommen, J., Grabmer, W., Thielmann, A., Schaub, A., Beauchamp, J., Wisthaler, A., and Hansel, A.: Eddy covariance flux measurements of biogenic VOCs during ECHO 2003 using proton transfer reaction mass spectrometry, Atmos. Chem. Phys., 5, 465–481, https://doi.org/10.5194/acp-5-465-2005, 2005

Stull, R. B.: An Introduction to Boundary Layer Meteorology (Atmospheric Sciences Library), Springer, 1988

Su, L. , Patton, E. G., Vilà-Guerau de Arellano, J., Guenther, A. B., Kaser, L., Yuan, B., Xiong, F., Shepson, P. B., Zhang, L., Miller, D. O., Brune, W. H., Baumann, K., Edgerton, E., Weinheimer, A., and Mak, J. E.: Understanding isoprene photo-oxidation using observations and modelling over a subtropical forest in the Southeast US. Atmos. Chem. Phys., 16, 7725-7741, https://doi.org/10.5194/acp-16-7725-2016, 2016

Sun, J.: Tilt correction over complex terrain and their implication for CO2-transport, Bound.-Lay. Meteorol., 124, 143–159, 2007

Sykes, R. I., Parker, S. F., Henna, D. S., and Lewellen,W. S.: Turbulent Mixing with Chemical Reaction in the Planetary Boundary Layer, J. Appl. Meteorol., 33, 825–834, 1994

van Stratum, B. J. H., Vilà-Guerau de Arellano, J., Ouwersloot, H. G., van den Dries, K., van Laar, T. W., Martinez, M., Lelieveld, J., Diesch, J.-M., Drewnick, F., Fischer, H., Hosaynali Beygi, Z., Harder, H., Regelin, E., Sinha, V., Adame, J. A., Sörgel, M., Sander, R., Bozem, H., Song, W., Williams, J., and Yassaa, N.: Case study of the diurnal variability of chemically active species with respect to boundary layer dynamics during DOMINO, Atmos. Chem. Phys., 12, 5329–5341, https://doi.org/10.5194/acp-12-5329-2012, 2012, 2012

Verver, G., van Dop, H., and Holtslag, A.: Turbulent mixing of reactive gases in the convective boundary layer, Bound.-Lay. Meteorol., 85, 197–222, 1997

Verver, G. H. L., van Dop, H., and Holtslag, A. A. M.: Turbulent mixing and the chemical breakdown of isoprene in the atmospheric boundary layer, J. Geophys. Res., 105, 3983–4002, 2000

Vilà-Guerau de Arellano, J., Duynkerke, P., and Builtjes, P.: The divergence of the turbulent diffusion flux in the surface layer due to chemical reactions: The NO-O3-NO2 system, Tellus, 43, 22–23, 1993

Vinuesa, J.-F. and J. Vila-Guerau de Arellano: Introducing effective reaction rates to account for the inefficient mixing of the convective boundary layer. Atmos. Environ., 39: 445–461, 2005

Wahrhaft, Z.: Passive scalars in turbulent flows, Annu. Rev. Fluid Mech., 32, 203–240, 2000

Wang, G., and Hendon, H. H.: Why 2015 was a strong El Niño and 2014 was not, Geophys. Res. Lett. 93, 63, https://doi.org/10.1002/2017GL074244, 2017

Wu, Z., Huang, N. E., Long, S. R., and Peng, C.-K.: On the trend, detrending, and variability of nonlinear and nonstationary time series. PNAS, 104, 14889 – 14894, https:// doi.org /10.1073/pnas.0701020104, 2007

Wyngaard, J.C.: Boundary- Layer Modelling. Lecture Notes on Atmospheric Turbulence and Air Polution Modelling, D. Riedel, Dordrecht, The Netherlands, Chap. 3, 1982

Wyngaard, J.C.: Structure of the atmospheric boundary layer and implications for its modeling. J. Climate Applied Meteorology, 24:1131 –1142, 1985

Wyngaard, J., and Brost, R. A.: Top-down and bottom-up diffusion of a scalar in the convective boundary layer. J. Atmos. Sci., 41, 102-112, https://doi.org/10.1175/1520-0469(1984)041<0102:TDABUD>2.0.CO;2, 1984

Yáñez-Serrano, A. M., Nölscher, A. C., Williams, J., Wolff, S., Alves, E., Martins, G. A., Bourtsoukidis, E., Brito, J., Jardine, K., Artaxo, P., and Kesselmeier, J.: Diel and seasonal changes of biogenic volatile organic compounds within and above an Amazonian rainforest, Atmos. Chem. Phys., 15, 3359-3378, https://doi.org/10.5194/acp-15-3359-2015, 2015

Zhou, M. Y., Lenschow, D. H., Stankov, B. B., Kaimal, J. C. and Gaynor, J. E.: Wave and turbulence structure in a shallow baroclinic convective boundary layer and overlying inversion, J. Atmos. Sci., 42, 47–57, https://doi.org/10.1175/1520-0469(1985)042<3C0047:WATSIA>3E2.0.CO;2, 1985